

The Application of BioHeat Perfusion Sensors to Analyze Preservation Temperature and Quantify Pressure Ischemia of Explanted Organs

Timothy J. O'Brien

Thesis submitted to the faculty of the Virginia Polytechnic Institute and State University in partial fulfillment of the requirements for the degree of

Master of Science
In
Mechanical Engineering

John L. Robertson, Co-Chair
Thomas E. Diller, Co-Chair
Rafael V. Davalos

February 19th, 2015
Blacksburg, Virginia

Keywords: Kidney, Transplant, Perfusion, Heat Flux, Temperature, Flow Rate

Copyright 2015

The Application of BioHeat Perfusion Sensors to Analyze Preservation Temperature and Quantify Pressure Ischemia of Explanted Organs

Timothy J. O'Brien

ABSTRACT

The development of an organ preservation system (primarily kidneys and livers, but could be adapted to fit hearts, lungs, and even limbs in the future) that can provide surgeons and doctors with real-time quantitative feedback on the health of the organ would be a significant improvement on current transplant practices. This organ transport system will provide surgeons and doctors the opportunity to make more educated decisions towards whether or not to proceed with organ transplantation. Here, we discuss the use Smart Perfusion's organ preservation system as a platform for determining the optimal perfusion temperature of an organ. Porcine kidneys were procured and perfused with a modified PBS solution on the Vasowave™. While on this organ preservation system, a heart emulating pressure waveform (90/50 mmHg) was generated and sent to the specimen. The pressure response, flow rate, temperature, pH, dissolved oxygen content, and conductivity of the fluid stream were all monitored throughout the duration of experimentation. In addition to inline sensors, IR imaging captured the surface temperature of the organ while on the system. Lastly, the use of a combined heat flux-temperature (CHFT) sensor, previously developed at Virginia Tech, was applied for the first time to monitor and measure local tissue perfusion of an explanted organ. A total of 12 experiments were performed (6 at a set fluid temperature of 15°C, and 6 at 20°C). All system data was collected, statistically evaluated and finally compared against blind histological readings (taken at the termination of each experiment at the hilum and pole) to investigate the effects of temperature on organ vasculature. The results of this experiment indicated that the effects of temperature on explanted kidneys can be affectively measured using a non-invasive bioheat perfusion sensor. Specifically, the lower temperature group of kidneys was measured to have lower perfusion. Furthermore, an enhancement to the CHFT sensor technology (CHFT+) was developed and tested for compliance. A controllable thin filmed heat resistor was added to the CHFT assembly to replace the current convective thermal event. This enhancement improved the measured heat flux and temperature signals and enables autonomy. Also, the thin and semi-flexible nature of the new CHFT+ sensor allows for perfusion measurements to be taken from the underside of the organ, permitting a quantitative measure of pressure ischemia. Results from a live tissue test illustrated, for the first time, the effects of pressure ischemia on an explanted porcine kidney.

Acknowledgements

I would like to express my sincere gratitude to all that played a part in making this project possible. First, I would like to thank Dr. John Robertson for his constant guidance, direction, encouragement, and most notably, for taking a chance on me and allowing me to achieve my true potential. I would also like to recognize Dr. Thomas Diller whose patience, and invaluable constructive criticism truly pushed me to new academic/ engineering heights. I feel blessed to have found such intelligent, kind-hearted co-advisors that could bring the best out of me. I am forever grateful for their mentorship. Similarly, I am very thankful for my third committee member, Dr. Rafael Davalos, for his collaboration, advice, and consistent support.

I'd like to acknowledge Smart Perfusion, LLC, specifically, George Barr and Don Faulkner for their continued support in this research and determination towards making a truly elite organ preservation system. Additionally, I'd like to thank Chip Aardema and Ali Roghanizad. Chip's experience with the Vasowave™ and procurement of organs were critical to the success of this project, while Ali's diligence and engineering tact was central in the manufacture of the CHFT+ sensor.

Lastly, I'd like to thank my parents, Theresa and Joseph O'Brien. Your support and encouragement has been a constant throughout my entire collegiate career. Everything that I have earned and achieved is in part due to your success as parents. I am extremely thankful for your attentive listening skills and patience. I love you both very much.

Preface

This Masters of Science thesis is organized into a manuscript format that includes two individual scientific papers that document the main focus of the work. The first chapter provides an introduction describing the main objectives. The first of the two papers (chapter 2) investigates the optimal perfusion temperature of explanted porcine kidneys, while the second paper (chapter 3) discusses the development of a non-invasive, thin-filmed surface perfusion sensor that could potentially be used to quantify pressure ischemia, amongst many other applications. Lastly, chapter 4 provides an overall conclusion of the work, as well as recommendations for future work. This is followed by a series of appendices which provides additional sensor manufacture information, as well as specific MATLAB and LabVIEW code.

Attribution

Chapter 2: The Analysis of Explanted Organ Perfusion to Determine Optimal Preservation Temperature

Timothy O'Brien¹, Charles Aardema^{1,3}, Thomas Diller¹, John Robertson^{1,2,3}

^[1] Virginia Tech Mechanical Engineering

^[2] Virginia Tech-Wake Forest School of Biomedical Engineering and Science

^[3] Smart Perfusion, LLC.

Charles Aardema helped in the procurement of porcine tissue, as well as organ preservation system preparation. Dr. Diller and Dr. Robertson both provided technical advice and guidance in experimental design. Dr. Robertson also performed a blind histological analysis on biopsy samples.

Chapter 3: The Development of a Thin-Filmed, Non-Invasive Tissue Perfusion Sensor to Quantify Pressure Ischemia of Explanted Organs

Timothy O'Brien¹, Ali Roghanizad¹, John Robertson^{1,2}, Thomas Diller¹

^[1] Virginia Tech Mechanical Engineering

^[2] Virginia Tech-Wake Forest School of Biomedical Engineering and Science

Ali Roghanizad aided in heat flux sensor calibration and the manufacture of the CHFT+ sensor. Dr. Diller provided technical advice and guidance on the manufacture of the sensor. Dr. Robertson was supportive on experimental design.

Table of Contents

CHAPTER 1 – INTRODUCTION	1
CHAPTER 2 – THE ANALYSIS OF EXPLANTED ORGAN PERFUSION TO DETERMINE OPTIMAL PRESERVATION TEMPERATURE	3
2.1 ABSTRACT	3
2.2 INTRODUCTION	4
2.3 ORGAN PRESERVATION TECHNOLOGIES	6
<i>2.3.1 Static Preservation</i>	<i>6</i>
2.3.1.1 Static Cold Storage (SCS).....	6
<i>2.3.2 Dynamic Preservation</i>	<i>8</i>
2.3.2.1 Hypothermic Machine Perfusion (HMP)	9
2.3.2.2 Normothermic Machine Perfusion (NMP)	9
2.3.2.3 Vasowave™ Organ Preservation System (VW).....	10
2.4 METHODOLOGY	13
<i>2.4.1 Experimental Design: Kidney Procurement and Preparation</i>	<i>14</i>
<i>2.4.2 Machine Perfusion of Explanted Organs</i>	<i>15</i>
<i>2.4.3 Non-Invasive Tissue Perfusion Measurements</i>	<i>17</i>
<i>2.4.4 Mathematical Model</i>	<i>22</i>
<i>2.4.5 Parameter Estimation</i>	<i>24</i>
2.5 RESULTS AND DISCUSSION	26
2.6 CONCLUSIONS	31
2.7 REFERENCES	33
CHAPTER 3 – THE DEVELOPMENT OF A THIN-FILMED, NON-INVASIVE TISSUE PERFUSION SENSOR TO QUANTIFY PRESSURE ISCHEMIA OF EXPLANTED ORGANS	39
3.1 ABSTRACT	39
3.2 INTRODUCTION	40

3.3 EXISTING PERFUSION MEASUREMENT TECHNOLOGIES	41
3.3.1 In-Depth Tissue Perfusion Methods.....	42
3.3.2 Surface Tissue Perfusion Methods.....	43
3.4 METHODOLOGY.....	44
3.4.1 Mathematical Model	44
3.4.1.1 System Model	44
3.4.1.2 Parameter Estimation	46
3.4.2 Manufacturing of CHFT+ Sensor.....	47
3.4.3 Controlled Phantom Tissue Testing	49
3.4.4 Explanted Porcine Kidney Testing	50
3.5 RESULTS & DISCUSSION.....	52
3.5.1 Phantom Tissue Testing.....	52
3.5.2 Live Tissue Testing.....	55
3.6 CONCLUSION.....	56
3.7 REFERENCES.....	58
CHAPTER 4 – CONCLUSIONS AND RECOMMENDATIONS	64
4.1 – CONCLUSIONS	64
4.2 – RECOMMENDATIONS.....	65
APPENDIX A – MATLAB CODE (PARAMETER ESTIMATION ROUTINE)	66
APPENDIX B – LABVIEW (HEAT FLUX AND TEMPERATURE MEASUREMENT).....	72
APPENDIX C – INSTRUCTIONS FOR MANUFACTURING THE CHFT+ SENSOR.....	73

List of Figures

FIGURE 1. DEMAND FOR KIDNEYS VS. TRANSPLANTS PERFORMED	5
FIGURE 2. STATIC COLD STORAGE BOX CONTAINING A STYROFOAM COOLER TO PRESERVE AND TRANSPORT A HUMAN KIDNEY.	7
FIGURE 3. COMPUTER GENERATED RENDERING OF SMART PERFUSION, LLC’S ORGAN PRESERVATION SYSTEM, THE VASOWAVE™.....	12
FIGURE 4. IMAGE OF A PORCINE KIDNEY FITTED WITH LURE-LOCK CONNECTORS.	14
FIGURE 5. (A) WORKING RESEARCH MODEL OF THE VASOWAVE™. (B) BASIC SYSTEM SCHEMATIC	16
FIGURE 6. COMPUTER GENERATED PRESSURE WAVEFORM SENT TO THE SPECIMEN ON THE VASOWAVE™.....	17
FIGURE 7. (A) CHFT SENSOR SCHEMATIC (B, C) CHFT SENSOR	18
FIGURE 8. (A) FRONT VIEW OF THE PHANTOM PERFUSION SYSTEM. (B) TOP VIEW DISPLAYING THE SPONGE USED ON THE PHANTOM PERFUSION SYSTEM.....	19
FIGURE 9. (A) SAMPLE HEAT FLUX CURVES. (B) SAMPLE TEMPERATURE CURVES.....	20
FIGURE 10. PORCINE KIDNEY WITH MARKED REGIONS FOR PERFUSION MEASUREMENTS.....	21
FIGURE 11. STEPWISE TEMPERATURE INPUT AS A FUNCTION OF TIME.....	23
FIGURE 12. (A) ERROR MINIMIZATION. (B) PARAMETER ESTIMATION SEARCH PROCESS SCHEMATIC.....	25
FIGURE 13. (A) PERFUSION COMPARISON OF VARYING SET PERFUSATE TEMPERATURES AT THE HILUM. (B) PERFUSION COMPARISON OF VARYING SET PERFUSATE TEMPERATURES AT THE POLE.....	27
FIGURE 14. AVERAGE FLOW RATE MEASURED FROM THE VENOUS LINE.....	28
FIGURE 15. (A) INFRARED IMAGE OF PORCINE KIDNEY. (B, C) IMAGE PROCESSING PROGRAM OUTPUT.	30
FIGURE 16. (A) COMPARISON OF THE KIDNEY SURFACE TEMPERATURE, VENOUS FLUID TEMPERATURE, AND CHFT ESTIMATE OF CORE TEMPERATURE FOR 15°C CASE. (B) COMPARISON OF THE KIDNEY SURFACE TEMPERATURE, VENOUS FLUID TEMPERATURE, AND CHFT ESTIMATE OF CORE TEMPERATURE FOR 20°C CASE.....	31
FIGURE 17. DEMAND FOR ORGANS.....	40
FIGURE 18. (A) ERROR MINIMIZATION. (B) PARAMETER ESTIMATION SEARCH PROCESS SCHEMATIC	46
FIGURE 19. (A) HEAT FLUX SENSOR (B) FOIL THERMOCOUPLE (C) RESISTIVE HEATING ELEMENT	47

FIGURE 20. CHFT+ SENSOR LAYERED ASSEMBLY SCHEMATIC	48
FIGURE 21. CHFT+ SENSOR.....	49
FIGURE 22. (A) FRONT VIEW OF THE PHANTOM PERFUSION SYSTEM. (B) TOP VIEW DISPLAYING THE SPONGE USED ON THE PHANTOM PERFUSION SYSTEM.....	49
FIGURE 23. (A) WORKING VASOWAVE™ RESEARCH MODEL (B) VASOWAVE™ FLOW SCHEMATIC (C) CARDIO-EMULATING PRESSURE WAVEFORM	50
FIGURE 24. SCHEMATIC ILLUSTRATING THE POSITIONING OF THE CHFT+ SENSOR BENEATH A PORCINE KIDNEY WITHIN THE VW ORGAN PRESERVATION SYSTEM.....	51
FIGURE 25. (A) PHANTOM TISSUE TESTING HEAT FLUX CURVES (B) PHANTOM TISSUE TESTING TEMPERATURE CURVES....	52
FIGURE 26. (A) HEAT FLUX CURVE FOR 25 CM ³ /MIN (B) TEMPERATURE CURVE FOR 25 CM ³ /MIN	53
FIGURE 27. COMPARISON OF PERFUSION ON THE TOPSIDE AGAINST THE UNDERSIDE	55
FIGURE 28. (A) INFRARED IMAGE OF PORCINE KIDNEY. (B, C) IMAGE PROCESSING PROGRAM OUTPUT.	56
FIGURE 29. (A) FRONT PANEL (B) BLOCK DIAGRAM.....	72
FIGURE 30. CHFT+ SENSOR LAYER ASSEMBLY SCHEMATIC	75

List of Tables

TABLE 1. PHANTOM TISSUE PERFUSION RESULTS WITH CHFT SENSOR20

TABLE 2. HISTOLOGICAL ANALYSIS OF EXPLANTED PORCINE KIDNEY VASCULATURE29

TABLE 3. PHANTOM TISSUE PERFUSION RESULTS WITH CHFT+ SENSOR.....54

TABLE 4. COMPARISON OF CHFT+ PERFUSION AND THE PENNES MODEL FROM MUDALIAR ET AL.54

List of Equations

[1].....	22
[2].....	23
[3].....	23
[4].....	45
[5].....	45
[6].....	45
[7].....	47

Chapter 1 – Introduction

The transport of thermal energy through blood flow within the body can be used to monitor important biological processes. Perfusion, the measure of flow through a volume of tissue at the capillary level, is critical in the delivery of nutrients, oxygen, and the removal of waste products. The ability to quantitatively measure perfusion has vast medical implications, such as, the severity of a burn wound, or the vascular response of an explanted organ to machine perfusion. Abnormal perfusion suggests that there may be a disruption or resistive element within the vascular bed. For the case of explanted organ studies, the occurrence of vasoconstriction due to cold perfusate temperatures, or the effect of pressure ischemia due to the weight of the organ could be revealed via the measurement of perfusion.

The measurement and evaluation of perfusion measurements on explanted organs is the main application investigated. According to the Organ Procurement and Transplant Network (OPTN), there are approximately 123,298 people in need of a life-saving organ transplant. Every 10 minutes, another name is added to that wait list. Unfortunately, approximately 21 people die each day while waiting. The organ supply deficit can be attributed to a number of elements including insufficient donation to meet the need, the discard of donated organs due to quality concerns, the inability to transplant due to time constraints of organs, and even surgical difficulties. Since the first kidney transplant performed in 1956, improvements in surgical techniques and the use of immunosuppressive medications have improved overall outcomes of transplant procedures. However, there still remain areas in which more can be done. Currently, the preferred method of organ preservation is static cold storage (SCS). This technology has remained the “gold standard” for organ preservation before implantation, mainly because it is a simple, low-cost solution, not necessarily because it is the best preservation method. An organ preservation system that may increase the supply of organs is in development at Virginia Tech. Smart Perfusion LLC’s Vasowave™ provides real-time monitoring of organ health. This system is capable of producing

and delivering any pressure waveform, while also maintains control of the perfusate temperature. Here, we utilized this system as a platform to support explanted porcine kidneys while non-invasive perfusion sensors were applied to measure the localized surface perfusion.

This dissertation consists of two papers under review for publication. The first paper investigates the effect of temperature on local perfusion measurements using a previously developed combined heat flux and temperature (CHFT) sensor. The results of this work showed that temperature the CHFT sensor provided repeatable perfusion information and could be used as a diagnostic tool for monitoring organ perfusion. Also, cold perfusate temperatures result in lower perfusion. The second paper introduces a novel, non-invasive, semi-flexible perfusion sensor (CHFT+) to be used to measure perfusion on any surface of an explanted organ. Preliminary results indicate that pressure ischemia may be factor in perfusion of the underside of an explanted organ.

Chapter 2 – The Analysis of Explanted Organ Perfusion to Determine Optimal Preservation Temperature

Timothy O'Brien¹, Charles Aardema^{1, 3}, Thomas Diller¹, John Robertson^{1, 2, 3}

^[1] Virginia Tech Mechanical Engineering

^[2] Virginia Tech-Wake Forest School of Biomedical Engineering and Science

^[3] Smart Perfusion, LLC.

2.1 Abstract

The development of an organ preservation system that provides real-time quantitative feedback on the health of the organ is an important goal in transplantation. This organ transport system will provide surgeons and doctors the opportunity to make more educated decisions towards whether or not to proceed with transplantation. Here, we discuss Smart Perfusion's organ preservation system (Vasowave™) as a platform for studying the optimal perfusion/preservation temperature for kidneys. Porcine kidneys were procured and perfused with modified PBS solution on the Vasowave™. A cardio-emulating pressure waveform (90/50 mmHg) was generated and sent to the specimen. The pressure response, flow rate, temperature, pH, dissolved oxygen content, and conductivity of the fluid stream were all monitored throughout the duration of experimentation. In addition, IR imaging recorded the surface temperature of the organ while on the system. During perfusion, a combined heat flux-thermocouple (CHFT) sensor, previously designed and developed to quantify the severity of burn wounds, was used to measure local tissue perfusion of the explanted kidney. These local perfusion measurements were then compared against closed-loop flow rate of fluid being circulated into and out of the organ. Tissue biopsy samples were taken at the end of each experiment and examined histologically to anatomically quantify the health of the explanted organ vasculature. A total of 12 experiments was performed (six at a set fluid temperature of 15°C, and six at 20°C). The results of this work verified the use of the non-invasive CHFT

sensor to tissue perfusion of an explanted porcine kidney and elucidate the response of organ vasculature to perfusate temperature.

Keywords: Organ, Perfusion, Temperature, Heat Flux

2.2 Introduction

Since the first kidney transplant in the early 1950s, improvements in surgical techniques and the use of immunosuppressive medications have resulted in better overall outcomes of transplant procedures. A workable technology, hypothermic, static cold storage (SCS) has been the preferred method of organ preservation mainly because it is a simple, low-cost method, with predictable results. It is not, however, necessarily optimum for organ preservation. SCS does not provide any sensing or measurements during the storage interval (termed “cold ischemia interval”) that predict organ success or chance of survival, forcing transplant surgeons to rely on gross organ appearance, a small biopsy, and consideration of donor and recipient characteristics. While hypothermic preservation has proven satisfactory for renal preservation (24-36 hrs.), the time frame from initial procurement to implantation is still much too short for other organs such as livers and hearts (6-12 hrs.). According to the Organ Procurement and Transplant Network (OPTN), as of January 1, 2015, there were 109,445 candidates on the Kidney Transplant Wait List. Unfortunately, fewer than 20% of them will likely receive a transplant. More than 2,600 kidneys are discarded annually (prior to transplantation) due to severe anatomical anomalies such as glomerulosclerosis, tubular atrophy, interstitial fibrosis, inflammation, cortical necrosis, vascular pathology, and prolonged cold and warm ischemic intervals (Orlando et al. 2013). Figure 1 summarizes the disparity of need against supply.

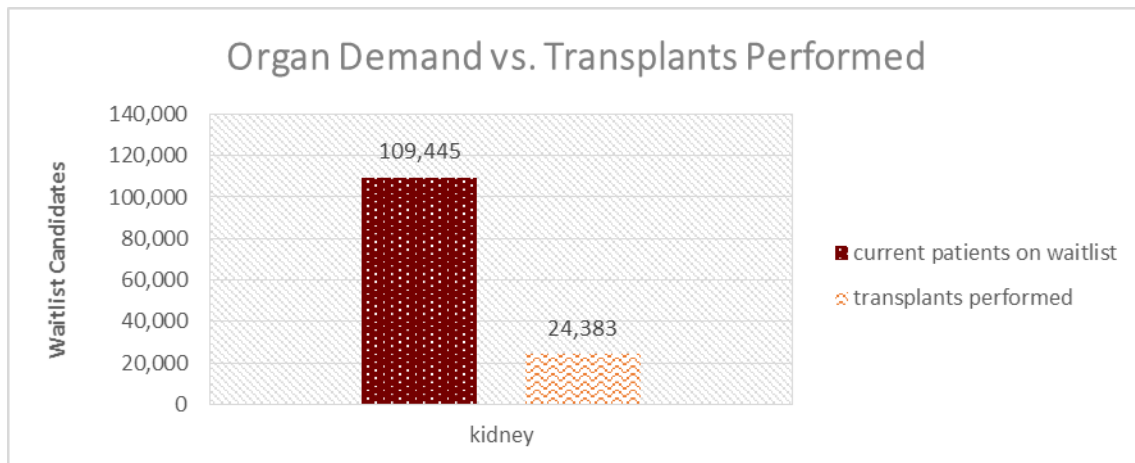


Figure 1. Demand for Kidneys vs. Transplants Performed

The shortfall in organ supply can be attributed to several factors, including insufficient donation to meet needs, discarding of organs before transplantation due to concerns over quality, inability to transplant in a timely manner, and problems occurring during surgery. For over 30 years, efforts to increase awareness of the importance of organ donation have had little effect on organ supply. Ways to significantly affect supply will be to manage the preservation of organs such that time is less of a factor, and to provide objective assessment of organ quality. An organ preservation system that may increase the supply of organs, as well as improve the overall quality of transplantable organs, is in development at Virginia Tech. Smart Perfusion’s Vasowave™ (VW) provides real-time organ vital sign monitoring over a wide range of temperatures. This cardio-emulating perfusion system is infinitely programmable to generate any blood pressure and waveform.

In the work reported here, the Vasowave™ system was utilized as the platform to support organ viability and collect vital data of explanted organs, while a non-invasive perfusion sensor was used to measure localized perfusion of the explanted organ. We hypothesized that the combined use of the Vasowave™ and the perfusion probe would provide doctors/ surgeons with advanced, predictive, knowledge of the overall health of the tissue when compared to larger database of healthy tissue metrics.

The goals of this research were to extend the knowledge-base on iterative prototypes of non-invasive perfusion sensing devices being used as a diagnostic tool in assessing explanted organ viability, as well as to analyze the effect of the fluid temperature on whole and localized organ perfusion.

2.3 Organ Preservation Technologies

The two modes of technology for organ preservation are static and dynamic preservation.

2.3.1 Static Preservation

The principle behind static organ preservation is to reduce the metabolic need of an explanted organ. This method is clinically approved for all organ types (kidney, liver, heart, and so forth) and has been the preferred method of choice since organ transplant came into existence (the 1970s).

2.3.1.1 *Static Cold Storage (SCS)*

Most organs are currently preserved by static cold storage (Yuan et al. 2010). After procurement from the donor, the organ is flushed by gravity with an organ preservation solution (typically Belzer UW solution or Celsior solution). Then, the organ is placed in a cooler of ice, such as shown in Figure 2, for cold storage and easy transportation. The hypothermic environment, as well as components in the perfusion solution, is used to reduce the metabolic activity.

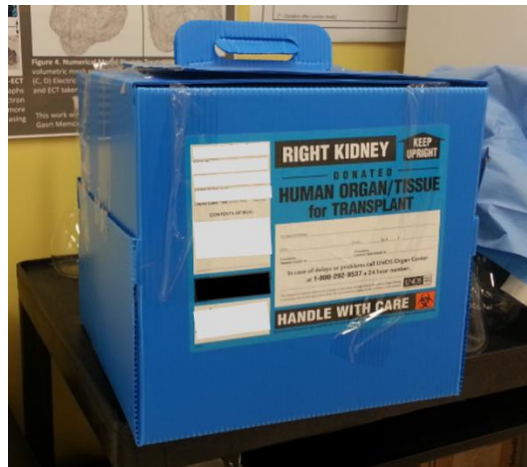


Figure 2. Static cold storage box containing a Styrofoam cooler to preserve and transport a human kidney.

According to Watson and Dark, static cold storage pushes the cells of the explant to “rapidly switch from aerobic to anaerobic metabolism, which requires 19 times more glucose substrate to generate adenosine triphosphate (ATP) than aerobic metabolism” (Watson and Dark 2012). This combination of rapid consumption of energy and accumulation of toxic metabolites and lactic acid ultimately results in a loss of cellular integrity- key factors in determining the critical times for implanting the organ. The organ, therefore, must be kept at hypothermic temperatures ($< 10^{\circ}\text{C}$) to slow cellular degradation (Watson and Dark 2012). While SCS has the advantage of being simple and facilitating easy transport from the donor to the recipient, it has been demonstrated that machine perfusion leads to better results. Moers *et al.* and Treckmann *et al.* have both verified that hypothermic machine perfusion not only reduced the risk of delayed graft function (DGF), but also improved graft survival within the first year following transplantation. Also, it has been shown that “different organs exhibit different tolerances to warm and cold ischemia” (Watson and Dark 2012). The heart, for example, has been shown to have the shortest tolerance to cold ischemia. Heart transplants should typically be performed within a 4 hour period. (Banner et al.) In contrast, kidneys show a much greater tolerance to cold ischemic conditions.

However, kidneys will fare better the sooner they are transplanted, the ideal time frame is within 18 hours.

While static cold storage is the most widely used technology for organ transportation and works reasonably well for renal transplants, there is simply too short of a preservation time frame for other organs, such as the heart and liver, to be procured from the donor, evaluated, transported and transplanted into the recipient. Also, SCS does not provide real-time numerical assessment of the organ quality that could predict – *before implantation* – the quality of organs. Without a means to objectively quantify organ viability, the only current way to find out if a transplant works is to place it in a person in organ failure and see if it “works”. The number of marginal, but actually functional organs that could have been used for transplantation but were ultimately discarded is unknown. A greater emphasis should be placed on obtaining a quantitative evaluation standard such that all suitable organs are used.

2.3.2 Dynamic Preservation

The principle behind dynamic organ preservation is to provide better nutrient delivery to the organ while also maintaining control over the preservation environment (Pressure, Temperature, Flow Rate, etc.) (Yuan et al. 2010). A consistent flow of perfusate throughout the organ can help to flush out residual blood and metabolic byproducts. This stimulation on the vasculature of the organ is vital to the functionality of the organ and has been shown to increase functionality of the organ after transplant in comparison to static preservation methods (Patel et al. 2012; Gallinat et al. 2012; Moers 2009; Treckmann et al. 2009). While exercising the vasculature (to maintain patency and structure) and continually providing the organ nutrients is essential to the overall health of the organ, the temperature of the preservation solution is equally important in maintaining the organ, as temperature can greatly influence the vasculature plasticity.

2.3.2.1 Hypothermic Machine Perfusion (HMP)

Hypothermic machine perfusion is an improvement upon the existing and widely used static cold storage method. It provides dynamic circulation of a preservation solution throughout the organ at sub-physiologic temperatures. In similar fashion to the ice used in static cold storage methods, the perfusate is administered to the organ at a hypothermic temperature (usually about 4°C) to reduce the metabolic demands and rate of organ cell death. This method of perfusion has been proven to reduce the risk of delayed graft function (DGF) and ultimately increases the odds of a positive post-transplantation, in comparison with static cold storage (Cannon et al. 2013). Although this system has shown some promising results, it has not gained wide clinical acceptance for several reasons. Primarily, most systems in place are only clinically approved for kidneys (not hearts or livers, for example). Virtually all HMP systems (Lifeport, Waters RM3) deliver a sinusoidal pressure waveform which does not emulate the pumping action of the human heart and this may impact on the vascular plasticity and the overall health of the organ. HMP systems do not provide any meaningful real-time monitoring of critical vital information, such as the pH of the perfusate throughout the system. It is hypothesized that the cold perfusion may induce undesirable vasoconstriction within the organ, creating a large resistance and ultimately shunting flow from capillaries. Consequently, while HMP systems have made improvements to the SCS method, there are still many avenues for improvement that would help overcome the shortage of transplantable organs (Yuan et al. 2010; Watson and Dark 2012).

2.3.2.2 Normothermic Machine Perfusion (NMP)

NMP is done when organs are perfused at or near physiologic temperature (37°C). This preservation concept is geared towards creating an environment that truly emulates the body and thus provides the organ both the chemical and physical setting it is most accustomed to. This method, in

contrast to the static cold storage and hypothermic machine perfusion methods, would “encourage” the organ to maintain its physiologic metabolism and subsequently reduce the formation and accumulation of toxic substrates. Given that oxygen and nutrients are amply supplied, and metabolic waste product removed, normothermic machine perfusion could allow for a strong real-time assessment of organ viability before committing the recipient to transplantation. Studies conducted by Valero and coworkers have shown that the use of normothermic machine perfusion on kidneys donated after cardiac death (DCD) have shown a “significant decrease in primary non-function and DGF in comparison to conventional preservation techniques”(Yuan et al. 2010; Valero et al. 2000). Like the other preservation methods, NMP also has its drawbacks. For example, the increase in temperature and subsequent rate of organ metabolism means that one must constantly maintain the pH of the perfusate and provide the organ the essential nutrients (especially oxygen) required in the body. This is not only difficult but also expensive.

2.3.2.3 Vasowave™ Organ Preservation System (VW)

Despite years of dedication towards enhancing organ preservation methods, the current technologies (HMP, NMP) are only minimally useful in terms of increasing the supply of transplantable organs, primarily being used for extended criteria organs (from elderly donors). There is a need for a medical device system that can improve the survival rate of organs outside of the body (the best known system for keeping organs alive is the body itself). Thus, the goal should be to improve upon existing technologies but also to build technology that supplies the physiologic demands that an organ would typically require *in vivo*. Such an “ideal” system should be modular and adaptable to meet the needs of various organ shapes, sizes, and types. The system should deliver a pressure waveform that accurately

simulates a pressure waveform generated by the heart. Furthermore, this system should provide transplant surgeons with real-time quantitative metrics to monitor and assess the health and functionality of the organ prior to transplantation. Such a system could overcome the shortage of transplantable organs with the evaluation and use of more donation after cardiac death (DCD) and marginal tissues. In addition, a prediction of the post-transplant viability could save the lives of potential recipients.

A machine perfusion system is in development that meets many of these needs. Smart Perfusion's Vasowave™ (VW) system has dramatically increased the lifespan of both kidneys and livers outside of the body in preclinical studies (Robertson, John. personal interview. 20 April 2013). This perfusion system is commonly referred to as a cardio-emulating perfusion system, as it is infinitely programmable to meet any pressure waveform and pulse, including to that found within the body. The VW system has been fabricated to control and monitor the perfusate temperature, while also monitoring organ-surface temperature via an infrared camera. Accordingly, with control over both the input pressure and perfusate temperature, this system is suitable for hypothermic and near normothermic preservation of several types of organs (kidneys and livers, for example). The VW system is capable of supplying the same or different pressure waveforms to multiple lines, such as the hepatic and portal veins of a liver. Additionally, the VW system was fabricated with the capacity to monitor vital sensory information, such as pH, dissolved oxygen, and conductivity, in real-time. A rendering of the Vasowave™ developed in Solid works is presented in Figure 3.



Figure 3. Computer generated rendering of Smart Perfusion, LLC's organ preservation system, the Vasowave™. <http://www.smartperfusion.com/vasowave.html>, used under fair use, 2015

Here, we utilize the VW organ preservation system as a platform to investigate the organ vascular response to different preservation temperatures via the use of a non-invasive tissue perfusion sensor. Tissue perfusion is defined as the quantity of fluid flow within a volume of tissue. Perfusion at the capillary level is critical to the transport of nutrients, oxygen, and the removal of waste product. Any disturbance in local perfusion could be the result of hypertension/hypotension, atherosclerosis, or gross anatomical abnormalities (such as tumors). Tissue perfusion sensing technology, like organ preservation systems, can be structured into two modes, namely deep tissue and surface measurement. Deep tissue measurement modes include Magnetic Resonance Imaging (MRI), Positron Emission Tomography (PET), Single Photon Emission Computer Tomography (SPECT), and Thermal Diffusion Probe (TDP). Laser Doppler Flowmetry (LDF), Laser Doppler Imaging (LDI), Doppler Ultrasound (DU), and Infrared Imaging (IR) all collectively make-up the surface measurement mode. Here, we have developed and

utilize another non-invasive tissue perfusion measurement system that was developed at Virginia Tech. This sensor, the combined heat flux and thermocouple (CHFT) sensor, originally designed to quantify the severity of burn wounds, is applied here as a diagnostic tool to measure localized perfusion of the explanted organ at various preservation temperatures (Al-khwaji, Vick, and Diller 2015).

Consequently, the combination of the Vasowave™ and the CHFT perfusion sensor could provide doctors/ surgeons with advanced, predictive, knowledge of the overall health of the tissue when compared to larger database of healthy tissue metrics.

2.4 Methodology

It was hypothesized that lower perfusate temperatures would result in lower tissue perfusion measurements due to the associated occurrence of vasoconstriction. To test this hypothesis, twelve explanted porcine organs were observed under machine perfusion of the Vasowave™ at two set fluid temperatures (15°C, 20°C). Another set of six organs were placed on static cold storage to act as a control group. It is important to note that the organs on the VW were provided a physiologic pressure waveform (90/50 mmHg). The pH, dissolved oxygen content, and the conductivity of the fluid stream were all measured via inline sensors integrated within the Vasowave™. The flow rate into and out of the organ, as well as, the surface temperature of the organ were collected. Moreover, localized tissue perfusion measurements were made external to the Vasowave™ using a combined heat flux and temperature (CHFT sensor) previously developed at Virginia Tech to better quantify the severity of burns (Al-khwaji, Vick, and Diller 2015; Alkhwaji, Vick, and Diller 2012). Tissue biopsy samples were taken at the termination of each experiment.

2.4.1 Experimental Design: Kidney Procurement and Preparation

Porcine kidneys were procured from a local abattoir and immediately fitted with Luer-Lock connectors and flushed at a constant pressure of ~90 mmHg with 1 liter of cold (4°C) modified PBS solution. During this period, the kidney was flipped on its alternate side every 250mL in an attempt to minimize pressure ischemia effects caused from the organ resting on a dense surface. Upon completion of the cold flush, the tissue was then placed on ice until anastomosed to the Vasowave™ organ preservation system at Virginia Tech. Figure 4 illustrates a porcine kidney that was fitted and prepped for the Vasowave™ organ preservation system. The red and white connectors are fastened to the artery and vein respectively. The yellow connector is connected to the ureter.

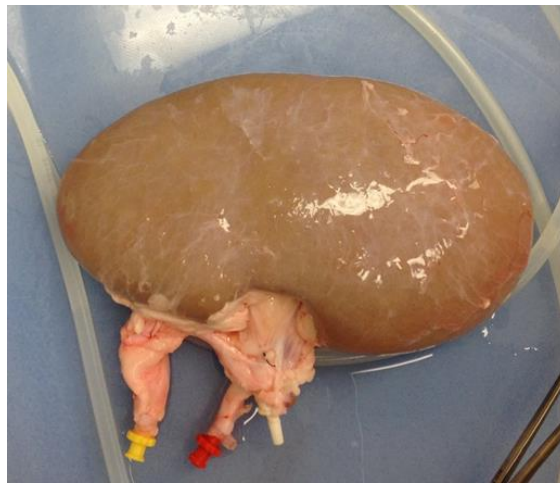


Figure 4. Image of a porcine kidney fitted with lure-lock connectors.

2.4.2 Machine Perfusion of Explanted Organs

Prior to connecting the organ to the Vasowave™, the system was rinsed, primed with modified PBS solution, and lastly de-bubbled. An image of the current working research model of the Vasowave™ is shown in Figure 5, complete with a schematic illustrating the flow direction. From the perfusate reservoir portion on the schematic, the fluid moves through a sensor block where pH, dissolved oxygen content, and conductivity probes are positioned to measure the fluid stream (Thermo Fisher Scientific, Waltham, MA). Following the sensor block, a BPX-80 BIO centrifugal pump drives the fluid through a BIOtherm heat exchanger (both developed by Medtronic, Minneapolis, MN) and to what is known as the pulse generator. This portion of the Vasowave™, developed by Smart Perfusion, LLC is considered the “heart” of the system, as this is where the physiologic waveform is physically created within the VW system. The waveform is generated via the delivery of controlled air pulses to a thin layer of expandable/deformable membranes within the pulse generator that then induce a hydraulic deformation and create the desired waveform. Immediately after the pulse generator, the perfusate passes through a SLQ-QT500 thermal flow sensor developed by Sensirion and connects to the specimen. This is fluid flow line is known as the arterial line. The perfusate stream continues through the organ and into a new line, the venous line, where the flow rate is again measured by another SLQ-QT500 thermal flow sensor. Lastly, the fluid stream is passed through the pulse generator and returned to the cassette directly over a drain leading to the fluid reservoir for recirculation.

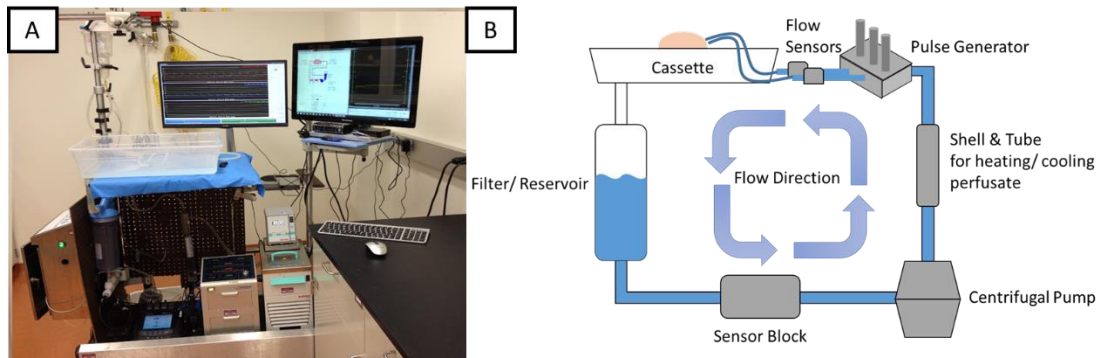


Figure 5. (A) Working research model of the Vasowave™. (B) Basic system schematic

Prior to connecting the organ to the system, the system is “de-bubbled”. These bubbles generate near the pump head, as well as the pulse generator. It’s important to ensure the removal of these from the fluid stream prior to connection of the organ to avoid sending these to the organ. It is equally important to remove gas bubbles since they could potentially create artifactual deformation of the pressure waveform by static expansion and collapse under pressure variance. Once the system was free of air bubbles, a physiologic pressure waveform was set and sent to the pulse generator. This waveform is depicted in figure 6. There is a clear rise in pressure, followed a slow decrease in pressure containing a slight indentation to resemble the dicrotic notch typically found in a physiologic pressure waveform. For each experiment, the diastolic and systolic pressures were set to 90 mmHg and 50 mmHg respectively. These values were chosen such that the explanted organs vasculature was not over pressurized.

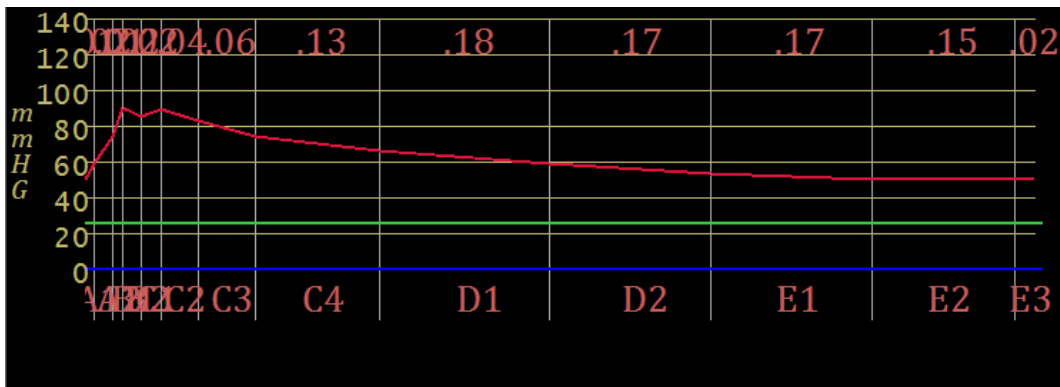


Figure 6. Computer generated pressure waveform sent to the specimen on the Vasowave™.

Then, the heater-cooler system was set to the desired fluid temperature (15°C or 20°C). Next, all of the other data capture devices (arterial flow, venous flow, infrared imaging, pH, dissolved oxygen, and conductivity) were set to record at the desired capture rate. Flow rate data was set to capture at a rate of 1 per second. Infrared Imaging was set to capture an image once every 15 minutes. All other inline data were set to capture at a rate of 1 per second. Lastly, the organ was introduced to the organ preservation system and the pump RPMs were slowly ramped up until the response pressure curve took the form of the previously set pressure waveform. This slow increase in pump revolution was performed as a preventative measure such that the organ vasculature was not “shocked” or damaged by forcing an initially high pressure on the previously ischemic tissue.

2.4.3 Non-Invasive Tissue Perfusion Measurements

The combined heat flux-temperature (CHFT) sensor is the main component of the bio-heat perfusion probe. The thermopile based heat-flux sensor is a BF-02 heat flux gage developed by Vatel, Corp with a sensitivity of 2.1 mV (W/cm²). The 10-mm x 10-mm sensor has a thickness of 0.25-mm. A foil thermocouple 0.0127-mm thick is laminated to the heat-flux gage. An air duct housing was

manufactured to distribute air onto the topside of the CHFT sensor creating a thermal event. Compressed air is driven to the air duct housing unit and through a matrix of nine 0.37-mm evenly spaced jet holes (Alkhwaji, Vick, and Diller 2012). Upon the activation of the compressed air, a sudden increase in heat transfer occurs from the tissue surface, through the thermal contact resistance layer, and across the CHFT device. A thin layer of plastic (Mylar) is placed over the specimen to reduce any evaporative effects that might result from a “weeping” organ. Figure 7 displays the sensor itself, as well as a schematic to better describe the data collection process.

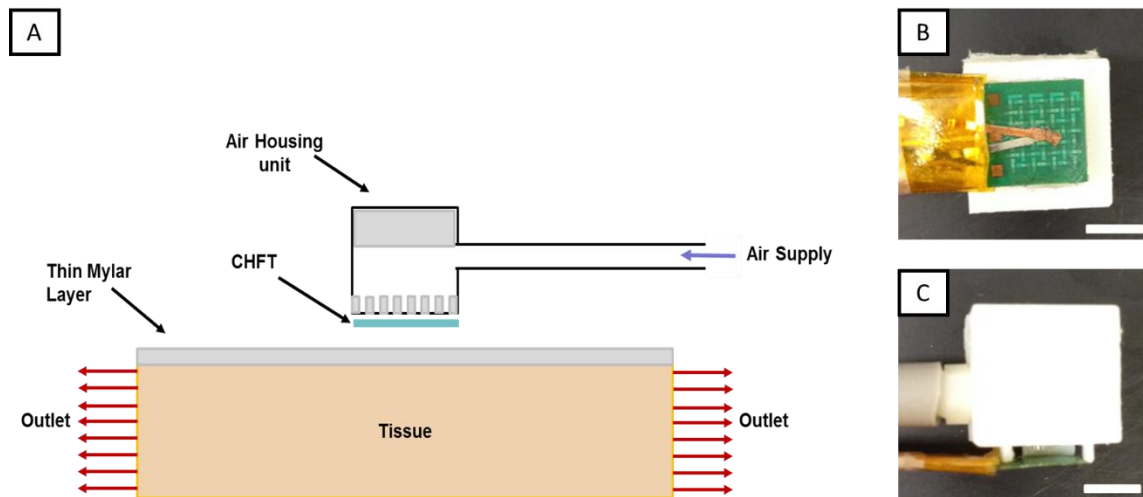


Figure 7. (A) CHFT Sensor Schematic (B, C) CHFT Sensor

Upon applying the CHFT sensor to the tissue surface, approximately 10 seconds of “non-thermal event” data is collected, followed by an additional 60 seconds of “thermal event” data. The resulting temperature and heat flux signals are collected via a 24-bit DAQ (capture rate of 1/second).

Prior to porcine tissue testing, preliminary experimental measurements were obtained using a Phantom Tissue System previously developed by Mudalier *et al.* to ensure that the sensor was working.

This test platform, shown in Figure 8, allows for the perfusion of a pseudo tissue (sponge) with control over both the fluid temperature and flow rate.

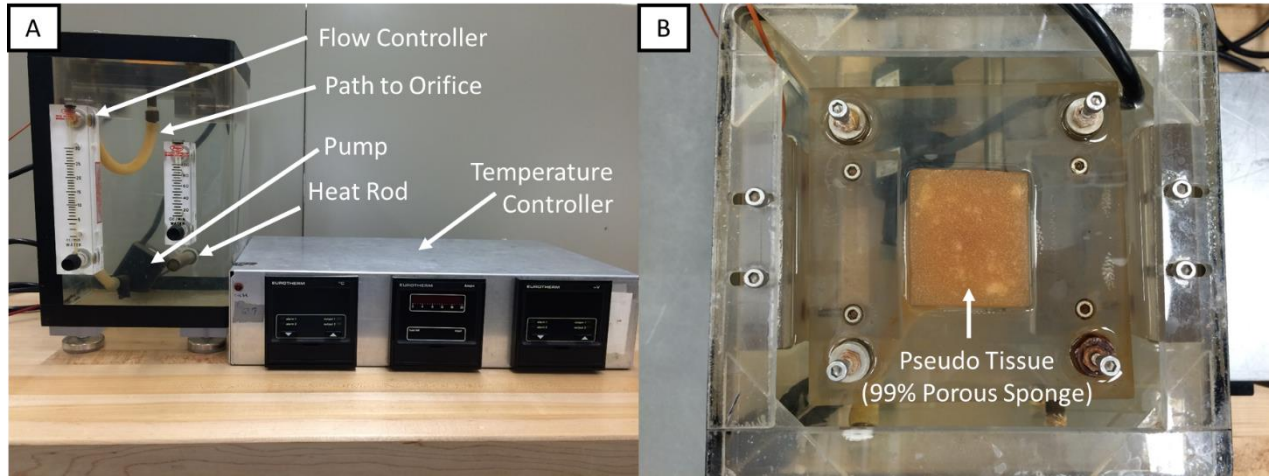


Figure 8. (A) Front view of the Phantom Perfusion System. (B) Top view displaying the sponge used on the Phantom Perfusion System

Figure 9 shows the results from preliminary data taken using the phantom perfusion system. Measured data was sent through a parameter estimation routine within MATLAB to analytically estimate the tissue perfusion based off a Pennes bio-heat equation model. The solid, blue line represents the measured data, while the dashed, red line represents the analytical solution. While the numerical and analytical heat flux curves should be close in comparison, the temperature curves should include some gap to account for the thermal contact resistance between the pseudo tissue and the CHFT sensor. Furthermore, it has been determined that higher heat flux curves represent higher perfusion. (Mudaliar et al. 2007) This particular sample was set to a temperature of 35°C, and a flow rate of 15 cm³/min.

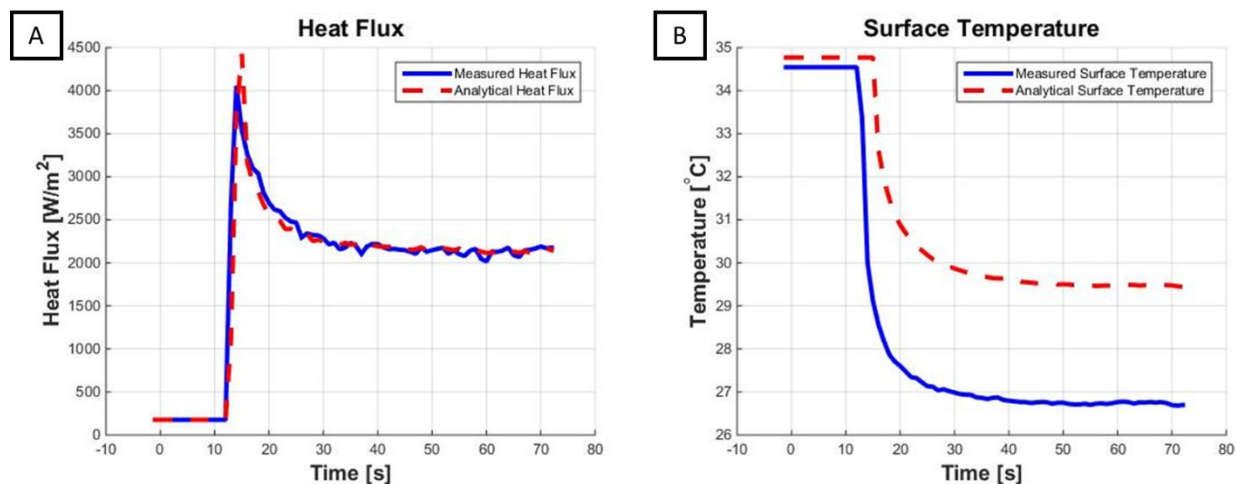


Figure 9. (A) Sample heat flux curves. (B) Sample temperature curves

Table 1 shows the preliminary results for each flow rate tested using the phantom perfusion system. The estimated perfusion values correlate well with set flow rates. As the set flow rate increases, the calculated tissue perfusion values also increase. The contact resistance and core temperature remain nearly the same, as expected in this controlled test.

Table 1. Phantom tissue perfusion results with CHFT sensor

Flow Rate [cm^3/min]	Contact Resistance [$m^2 \cdot K/W$]	Tissue Perfusion [ml/ml/s]	Core Temperature [°C]	Error
5	0.001227	0.03642	35.0609	201.1439
15	0.001279	0.06374	35.2512	220.1072
30	0.001299	0.16688	36.0738	196.4347

Once introduced to the system, each kidney was continually monitored over the subsequent 12-hours. Pressure response, arterial and venous line flow rates, and surface temperature, as well as the fluid

temperature, pH, dissolved oxygen content, and conductivity were all measured autonomously, while the CHFT sensor required manual operation. The CHFT sensor was utilized on explanted porcine organs to measure the localized tissue perfusion at the capillary level at two different regions on each kidney, at the hilum and a pole. A thin layer of Mylar is placed over the top-side of the organ for perfusion measurements. Each region is marked on the Mylar to enable consistent measurement location, as shown in Figure 10.

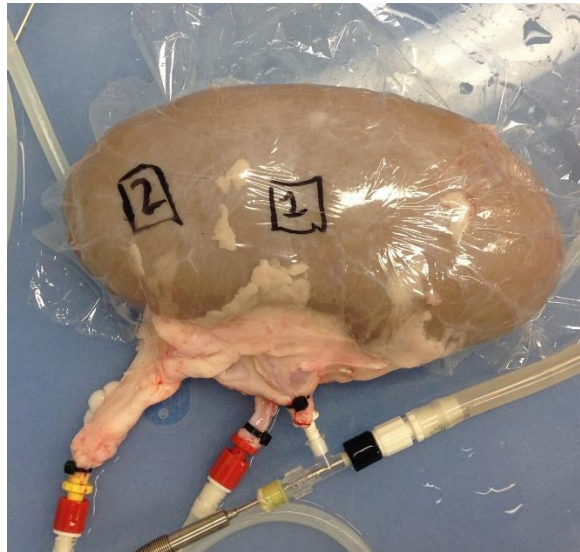


Figure 10. Porcine Kidney with marked regions for perfusion measurements

Three measurements at each region were taken and averaged at five different time points over the 12 hour experiment.

2.4.4 Mathematical Model

Originally developed to predict the heat transfer of a human forearm, the Pennes bio-heat equation has since been used to model various biological tissues due to its accurate, yet simplistic form. The model inherently assumes homogenous tissue properties and uniform metabolic heat generation and distribution. The model also assumes there is proportionality between the convective heat transfer from the perfusate (blood) to the tissue and the temperature difference between the arterial fluid entering the tissue and the venous flow leaving the tissue (Pennes 1948). Here, we have used Pennes bio-heat equation to model the perfusion of the outer cortex of an explanted porcine kidney. Two additional assumptions were made to better define this particular model. The first being the assumption of one dimensionality due to the thermal penetration depth being small in comparison to both the width and length of the sensor during the thermal event. The second assumption is the neglect of metabolic heat generation as it is also deemed small in comparison to the measured heat flux. Thus, the Pennes bio-heat equation for this particular model reduces to the form illustrated in equation 1, where ρ is the density, c is the heat capacitance, w is the perfusion, T is the temperature of the surface, T_{core} is the core temperature, k is the thermal conductivity of the tissue, t is time, and x is the direction of the heat transfer.

$$(\rho c)_p \frac{\partial T}{\partial t} = k \frac{\partial^2 T}{\partial x^2} - (\rho c w)_b (T - T_{core}) \quad [1]$$

The measured sensor temperature profile is modeled as a series of steps.

$$\theta_s(t) = \theta_s(0) + \sum_{n=1}^{Nmax} \Delta\theta_{s,n} \cdot H(t - t_n) \quad [2]$$

Where $\theta = (T - T_{core})$ and $H(t)$ is the step function. A visual representation of the temperature input is shown in Figure 11.

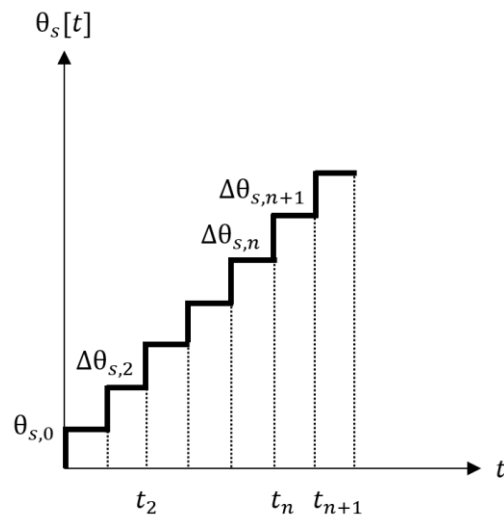


Figure 11. Stepwise temperature input as a function of time

Thus, in terms of the variable $\theta(x, t) = T(x, t) - T_{core}$ the bio-heat equation becomes

$$(\rho c)_p \frac{\partial \theta}{\partial t} = k \frac{\partial^2 \theta}{\partial x^2} - (\rho c w)_b \theta \quad [3]$$

2.4.5 Parameter Estimation

The objective of any parameter estimation routine is to find a combination of unknown system parameters that minimize the sum of the squares of the residuals between the measured experimental data and theoretical predictions. For this specific model, there are three unknown physical system parameters: the core temperature of the specimen, tissue perfusion, and the thermal contact resistance between the sensor and the tissue surface. These parameters must be determined from the measured temperature and heat flux. Because each physical parameter is highly dependent upon one another, the estimation of these parameters is a highly iterative process. The best fit analytical model is when the error is driven to a minimum. Figure 12 provides a visual explanation of this error minimization process, where error is denoted by the variable S (Alkhwaji, Vick, and Diller 2012). To minimize the error, two of the system parameters (contact resistance and blood perfusion) are varied one at a time over a range of values to iteratively arrive at the minimum. First the contact resistance is held constant while varying the blood perfusion. Then, the best value of the blood perfusion is used while varying the contact resistance. This hold and vary routine is repeated over finer and finer ranges until a sufficient resolution has been achieved.

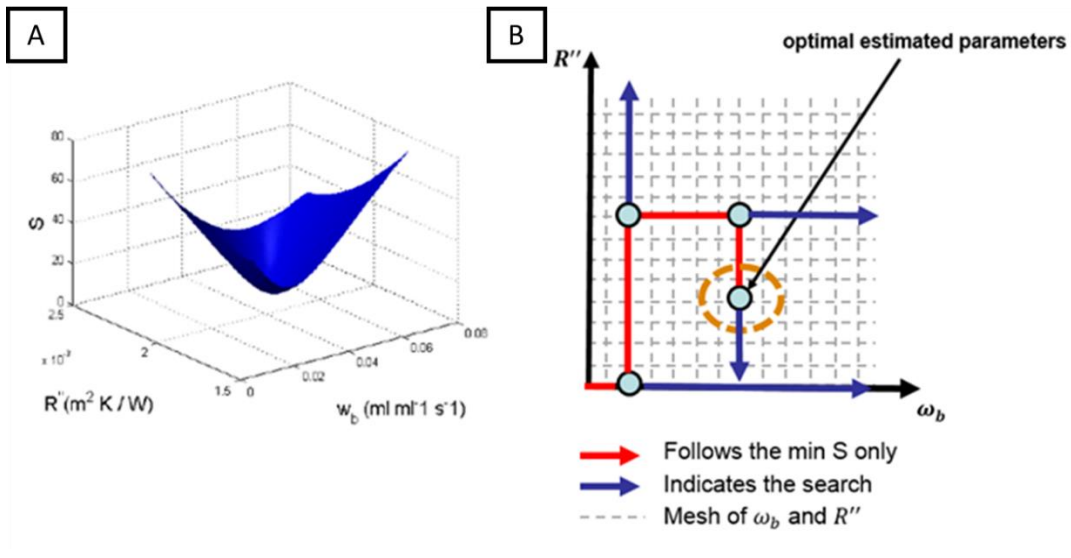


Figure 12. (A) Error Minimization. (B) Parameter Estimation Search Process Schematic

The third and final unknown system parameter, core temperature, is initially calculated using the measured steady state values. Then, throughout the parameter estimation routine, for each new parameter value used, a new core temperature value is calculated using the equation #.

$$T_{core} = T_{s,o} + \frac{q_{s,o}}{\left[\frac{k\sqrt{w_b/\alpha}}{1 + R'' k\sqrt{w_b/\alpha}} \right]} \quad [4]$$

2.5 Results and Discussion

It was hypothesized that the vasculature of the explanted organs preserved at sub-normothermic temperatures would undergo vasoconstriction and thus experience a lower perfusion at the capillary level. Lower perfusate temperature equates to a lower the perfusion due to the high resistance caused by the vasoconstriction.

Figure 13 illustrates the perfusion trends at each region for the one sample set of kidneys with a focus on the comparison between initially set perfusate temperatures. Evaluating the perfusion trends at region 1, both temperatures show similar perfusion trends, with slight deviation at the beginning of the experiment. Both trends appear to be relatively steady between 0.015 and 0.025 ml/ml/s. The same is true at region 2, where both regions display a similar trend over the 12-hour experiment, with deviation at the beginning and again at the 10th hour. It is clear that the set perfusate temperature 20°C perfusion trend is higher than the 15°C perfusion trends for both regions, agreeing with the initial hypothesis.

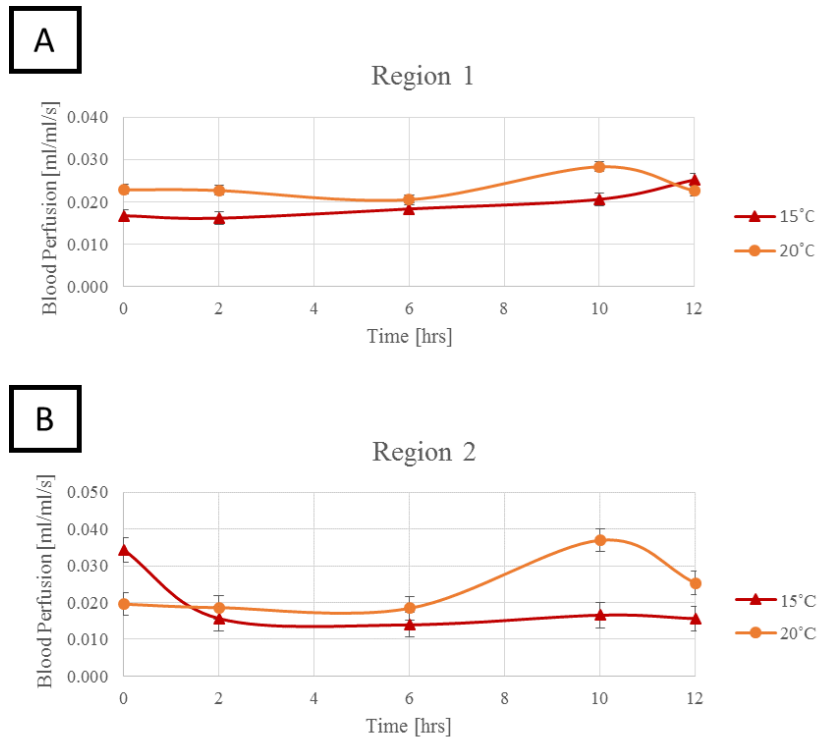


Figure 13. (A) Perfusion comparison of varying set perfusate temperatures at the hilum. (B) Perfusion comparison of varying set perfusate temperatures at the pole.

Comparing these perfusion results to the flow exiting the organ, both show that higher temperature preservation results in a higher flow rate through explanted porcine kidneys. The venous flow for both the 15°C and 20°C data sets are shown in Figure 14.

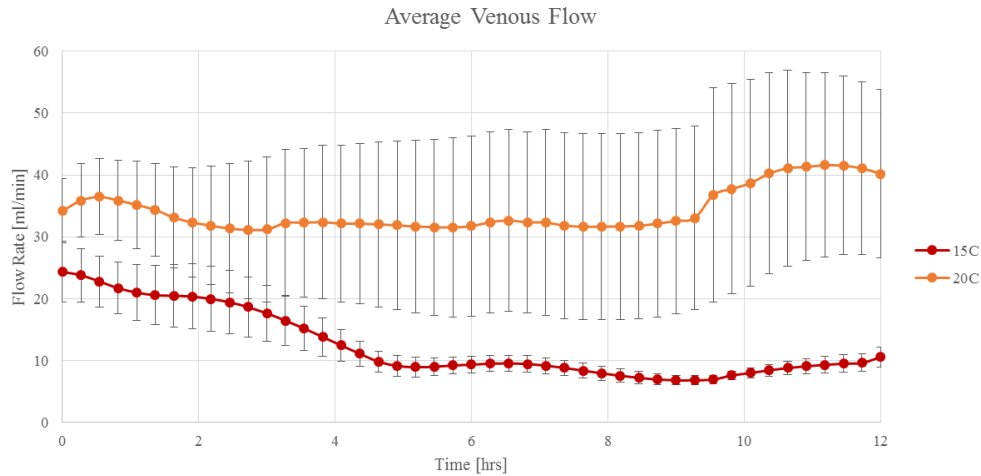


Figure 14. Average flow rate measured from the venous line

Results from the histological analysis were in agreement with the perfusion and flow results as well. Table 1 displays the results. Here a ‘+’ rating system was applied to indicate the severity of the condition. A ‘+’ represents a minimal severity, ‘++’ indicates a mild severity, ‘+++’ signifies a moderate severity, and ‘++++’ is substantial severity. The higher temperature samples showed the most amount of tissue degeneration or autolysis and slightly more tubular dilation. In other words, these results qualitatively indicate that the 20°C kidneys had slightly more fluid flow throughout the tubules than the 15°C set. However, the higher temperature greatly impacted the severity of tissue degradation and possibly the integrity of the vascular bed by the end of the experiments.

Table 2. Histological analysis of explanted porcine kidney vasculature

Test	Date of Exp.	Fluid Temp	Degeneration/ Autolysis	Tubular Dilation	Mineral Deposits	Inflammation of cells	Not remarkable
n1	08.26.2014	Control (SCS)	++ diffuse	+	-	-	
n2	09.04.2014	Control (SCS)	-	-	+	-	NR
n3	09.09.2014	Control (SCS)	-	-	-	-	NR
n4	09.11.2014	Control (SCS)	-	-	-	-	NR
n5	09.16.2014	Control (SCS)	-	-	-	-	NR
n6	09.18.2014	Control (SCS)	-	-	-	-	NR
n1	11.05.2014	15	-	-	-	+	NR
n2	11.06.2014	15	-	+++	-	-	
n3	11.07.2014	15	++ multifocal	++	+	-	
n4	11.11.2014	15	-	+++	++	-	
n5	11.12.2014	15	+++ patchy	-	-	P	
n6	11.13.2014	15	+++	-	-	-	
n1	11.19.2014	20	+++ patchy	-	-	-	
n2	11.20.2014	20	+++ diffuse	+++	-	-	
n3	11.21.2014	20	+++ diffuse	-	+++	-	
n4	12.02.2104	20	-	++	-	-	NR
n5	12.04.2014	20	++++ diffuse	-	+	-	
n6	12.05.2014	20	++	-	++	-	

Additionally, the core temperature estimated from the parameter estimation routine was compared against the surface temperature and the fluid temperature directly exiting the vein. Thermal images taken during the course of experimentation were processed through MATLAB to determine the average surface temperature of the kidney. A standard search routine was implemented within the image processing program to ensure that the averaged surface temperature data only included that of the kidney itself and not any surrounding material. Figure 15 shows a sample of a processed infrared image, the region which was found via the search routine, and the resulting average surface temperature output over the course of the 12-hr experiment.

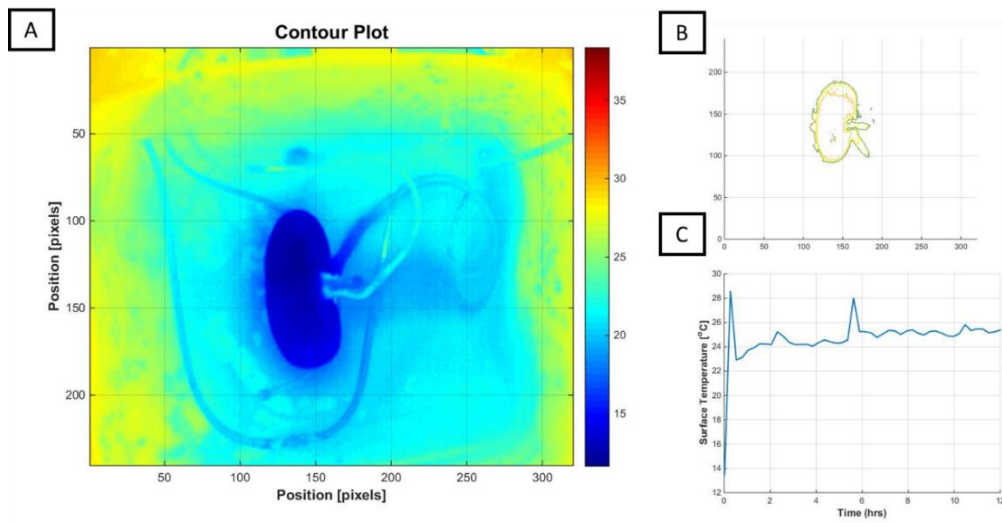


Figure 15. (A) Infrared image of porcine kidney. (B, C) Image processing program output.

The temperature of the fluid immediately exiting the tissue was measured as well using an inline thermal temperature probe. This measurement provided an approximation for what the actual core temperature of the kidney was. The surface temperature of the organ showed the higher temperature than the venous fluid temperature, indicating a temperature gradient across the cortex of the kidney. The average temperature differences between the kidney surface temperature and the venous fluid temperature were 3.38°C and 3.29°C for the 15°C and 20°C experimental cases respectively. Then the CHFT sensor's estimate for core temperature was evaluated for accuracy against the measured fluid and surface temperatures. Figure 16 displays this comparison for both the 15°C and 20°C cases. The estimated core temperature was no more than 2°C off from the measured fluid and surface temperatures, signifying a good estimation.

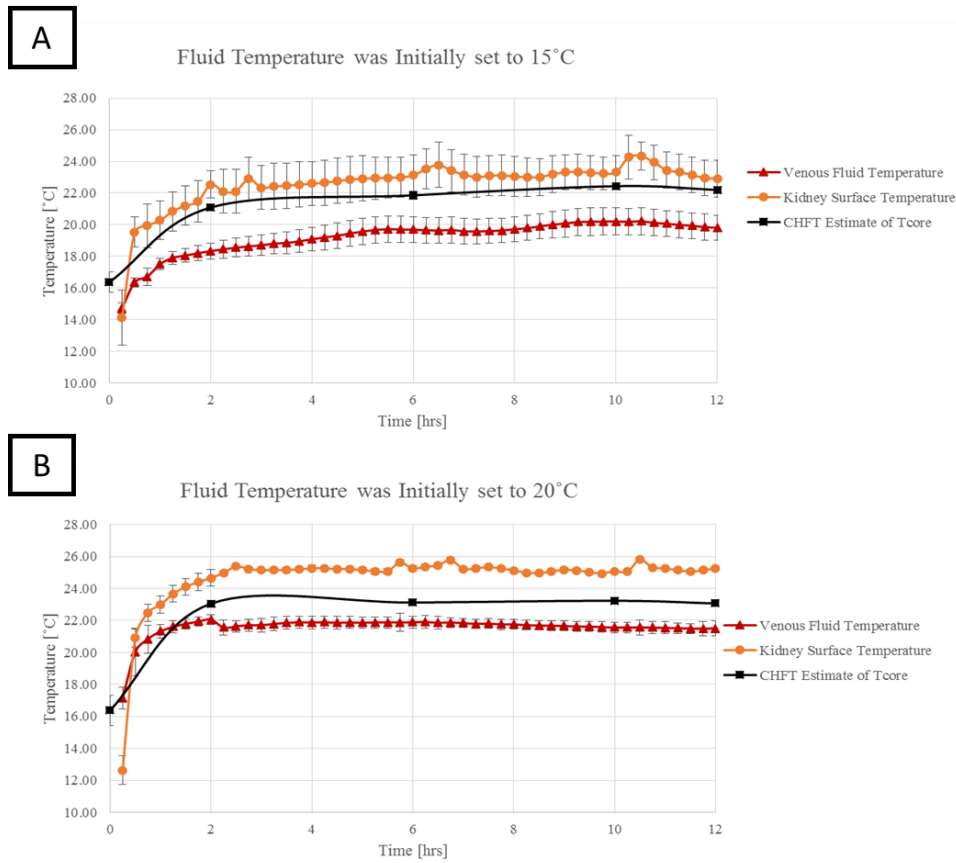


Figure 16. (A) Comparison of the kidney surface temperature, venous fluid temperature, and CHFT estimate of core temperature for 15°C case. (B) Comparison of the kidney surface temperature, venous fluid temperature, and CHFT estimate of core temperature for 20°C case.

2.6 Conclusions

This study demonstrated proof-of-concept for the use of a non-invasive perfusion sensor on explanted organs and correlated several heat measurements (CHFT, direct measurement of perfusate temperature, IR imaging) with the viability of porcine kidneys at different perfusate temperatures. The combined heat flux and temperature (CHFT) sensor was shown to provide repeatable perfusion information that agreed with flow measurements when applied to explanted porcine kidneys. This data indicated that porcine kidney vasculature was sensitive to perfusate temperature; even at the capillary level. Additionally, this perfusion and flow data in combination with histological analysis specified that

while the organ vasculature experienced vasodilation for the higher temperatures, the tissue also degraded much more significantly over time. Understanding the temperature response of explanted organs could lead to longer preservation periods, lessening the time constraint that transplant surgeons typically have to work within, as well as improving post-transplant graft survival.

Future studies should be performed at a much larger temperature range to better identify the optimal preservation temperature. Also, organs procured in-house and immediately placed on the Vasowave™ organ preservation system at the desired perfusate temperature. Lastly, a more chemically stable perfusate, such as a Belzer UW solution for the lower temperatures and an oxygen carrying solution for the higher temperature experiments should be used to ensure that the organ is provided all essential nutrients for that specific temperature range.

2.7 References

- Alkhwaji, Abdusalam, Brian Vick, and Tom Diller. 2012. "New Mathematical Model to Estimate Tissue Blood Perfusion, Thermal Contact Resistance and Core Temperature." *Journal of Biomechanical Engineering* 134 (8): 081004. doi:10.1115/1.4007093.
- Al-khwaji, Abdusalam, Brian Vick, and Tom Diller. 2015. "Modeling and Estimating Simulated Burn Depth Using the Perfusion and Thermal Resistance Probe" 7 (September 2013): 1–9. doi:10.1115/1.4024160.
- Badea, C T, M Drangova, D W Holdsworth, and G a Johnson. 2008. "In Vivo Small-Animal Imaging Using Micro-CT and Digital Subtraction Angiography." *Physics in Medicine and Biology* 53: R319–50. doi:10.1088/0031-9155/53/19/R01.
- Boellaard, Ronald, Paul Knaapen, Abraham Rijbroek, Gert J J Luurtsema, and Adriaan a. Lammertsma. 2006. "Evaluation of Basis Function and Linear Least Squares Methods for Generating Parametric Blood Flow Images Using 15O-Water and Positron Emission Tomography." *Molecular Imaging and Biology* 7 (August): 273–85. doi:10.1007/s11307-005-0007-2.
- Cannon, Robert M., Guy N. Brock, R. Neal Garrison, Jason W. Smith, Michael R. Marvin, and Glen a. Franklin. 2013. "To Pump or Not to Pump: A Comparison of Machine Perfusion vs Cold Storage for Deceased Donor Kidney Transplantation." *Journal of the American College of Surgeons* 216 (4). Elsevier Inc: 625–34. doi:10.1016/j.jamcollsurg.2012.12.025.
- Detre, Ja - Google. 2008. "Traduzido - Arterial Spin Labeled Perfusion Mri." *Clinical Neurology*, 6–12. http://usa.healthcare.siemens.com/siemens_hwem-hwem_sxxa_websites-context-root/wcm/idc/groups/public/@us/@clinicalspec/documents/download/mdaw/nde3/~edisp/magneto_m_mr-clinical-cases-asl-case-00305305.pdf.

- Gallinat, Anja, Cyril Moers, Jürgen Treckmann, Jacqueline M. Smits, Henry G D Leuvenink, Rolf Lefering, Ernest Van Heurn, et al. 2012. “Machine Perfusion versus Cold Storage for the Preservation of Kidneys from Donors ≥ 65 Years Allocated in the Eurotransplant Senior Programme.” *Nephrology Dialysis Transplantation* 27 (July): 4458–63. doi:10.1093/ndt/gfs321.
- Khot, Monica B, Peter K M Maitz, Benjamin R Phillips, H Frederick Bowman, Julian J Pribaz, and Dennis P Orgill. 2005. “Thermal Diffusion Probe Analysis of Perfusion Changes in Vascular Occlusions of Rabbit Pedicle Flaps.” *Plastic and Reconstructive Surgery* 115: 1103–9. doi:10.1097/01.PRS.0000156546.45229.84.
- Majchrzak, Ewa. “3d Thermal Wave Model of Bioheat Transfer - Solution by Means of Finite Difference Method,” no. 2.
- Moers, Cyril et al. 2009. “New England Journal.” *The New England Journal of Medicine*, 1495–1504.
- Monstrey, Stan, Henk Hoeksema, Jos Verbelen, Ali Pirayesh, and Phillip Blondeel. 2008. “Assessment of Burn Depth and Burn Wound Healing Potential.” *Burns* 34: 761–69. doi:10.1016/j.burns.2008.01.009.
- Montet, Xavier, Marko K Ivancevic, Jacques Belenger, Manuel Jorge-Costa, Sybille Pochon, Antoinette Pechère, François Terrier, and Jean-Paul Vallée. 2003. “Noninvasive Measurement of Absolute Renal Perfusion by Contrast Medium-Enhanced Magnetic Resonance Imaging.” *Investigative Radiology* 38 (9): 584–92. doi:10.1097/01.RLI.0000077127.11949.8c.
- Mudaliar, Ashvinikumar V, Thomas E Diller, D Sc, Elaine P Scott, Ph D Co-chair, Otto I Lanz, Diplomate Acvs, Danesh Tafti, D Ph, and Brian Vick. 2007. “Development of a Phantom Tissue for Blood Perfusion Measurement and Noninvasive Blood Perfusion Estimation in Living Tissue Virginia Polytechnic Institute and State University in Partial Fulfillment of the Requirements for the Degree of Doctor of Philosop.”

- Mudaliar, Ashvinikumar V, Brent E Ellis, Patricia L Ricketts, Otto I Lanz, Charles Y Lee, Thomas E Diller, and Elaine P Scott. 2008. "Noninvasive Blood Perfusion Measurements of an Isolated Rat Liver and an Anesthetized Rat Kidney." *Journal of Biomechanical Engineering* 130 (6): 061013. doi:10.1115/1.2978989.
- Mudaliar, Ashvinikumar V, Brent E Ellis, Patricia L Ricketts, Otto I Lanz, Elaine P Scott, and Thomas E Diller. 2008. "A Phantom Tissue System for the Calibration of Perfusion Measurements." *Journal of Biomechanical Engineering* 130 (October 2008): 051002. doi:10.1115/1.2948417.
- Nett, Brian E, Robert Brauweiler, Willi Kalender, Howard Rowley, and Guang-Hong Chen. 2010. "Perfusion Measurements by Micro-CT Using Prior Image Constrained Compressed Sensing (PICCS): Initial Phantom Results." *Physics in Medicine and Biology* 55: 2333–50. doi:10.1088/0031-9155/55/8/014.
- Niwayama, Jun, and Tsutomu Sanaka. 2005. "Development of a New Method for Monitoring Blood Purification: The Blood Flow Analysis of the Head and Foot by Laser Doppler Blood Flowmeter during Hemodialysis." *Hemodialysis International. International Symposium on Home Hemodialysis* 9: 56–62.
- Nuutila, P, and K Kalliokoski. 2000. "Use of Positron Emission Tomography in the Assessment of Skeletal Muscle and Tendon Metabolism and Perfusion." *Scandinavian Journal of Medicine & Science in Sports* 10: 346–50.
- Oltean, M, a Aneman, G Dindelegan, J Mölne, M Olausson, and G Herlenius. 2005. "Monitoring of the Intestinal Mucosal Perfusion Using Laser Doppler Flowmetry after Multivisceral Transplantation." *Transplantation Proceedings* 37 (8): 3323–24. doi:10.1016/j.transproceed.2005.09.032.

- Orlando, Giuseppe, Christopher Booth, Zhan Wang, Giorgia Totonelli, Christina L. Ross, Emma Moran, Marcus Salvatori, et al. 2013. "Discarded Human Kidneys as a Source of ECM Scaffold for Kidney Regeneration Technologies." *Biomaterials* 34 (24). Elsevier Ltd: 5915–25. doi:10.1016/j.biomaterials.2013.04.033.
- Patel, S K, O G Pankewycz, N D Nader, M Zachariah, R Kohli, and M R Laftavi. 2012. "Prognostic Utility of Hypothermic Machine Perfusion in Deceased Donor Renal Transplantation." *Transplantation Proceedings* 44 (7). Elsevier Inc.: 2207–12. doi:10.1016/j.transproceed.2012.07.129.
- Pennes, Hh. 1948. "Analysis of Tissue and Arterial Blood Temperatures in the Resting Human Forearm." *Journal of Applied Physiology*, 5–34. doi:9714612.
- Petersson, Johan, Alejandro Sánchez-Crespo, Malin Rohdin, Stéphanie Montmerle, Sven Nyrén, Hans Jacobsson, Stig a Larsson, et al. 2004. "Physiological Evaluation of a New Quantitative SPECT Method Measuring Regional Ventilation and Perfusion." *Journal of Applied Physiology (Bethesda, Md. : 1985)* 96 (November 2003): 1127–36. doi:10.1152/jappphysiol.00092.2003.
- Prinzen, Frits W., and James B. Bassingthwaite. 2000. "Blood Flow Distributions by Microsphere Deposition Methods." *Cardiovascular Research* 45: 13–21. doi:10.1016/S0008-6363(99)00252-7.
- Schelbert, Heinrich R. 2000. "PET Contributions to Understanding Normal and Abnormal Cardiac Perfusion and Metabolism." *Annals of Biomedical Engineering* 28: 922–29. doi:10.1114/1.1310216.
- Svedman, Cecilia, George W. Cherry, Elizabeth Strigini, and Terence J. Ryan. 1998. "Laser Doppler Imaging of Skin Microcirculation." *Acta Dermato-Venereologica* 78: 114–18. doi:10.1080/000155598433430.

- Treckmann, Jürgen, Manfred Nagelschmidt, Thomas Minor, Fuat Saner, Stefano Saad, and Andreas Paul. 2009. "Function and Quality of Kidneys after Cold Storage, Machine Perfusion, or Retrograde Oxygen Persufflation: Results from a Porcine Autotransplantation Model." *Cryobiology* 59 (1). Elsevier Inc.: 19–23. doi:10.1016/j.cryobiol.2009.03.004.
- Valero, R, C Cabrer, F Oppenheimer, E Trias, J Sánchez-Ibáñez, F M De Cabo, a Navarro, et al. 2000. "Normothermic Recirculation Reduces Primary Graft Dysfunction of Kidneys Obtained from Non-Heart-Beating Donors." *Transplant International : Official Journal of the European Society for Organ Transplantation* 13 (4): 303–10.
- Valvano, J W, J T Allen, and H F Bowman. 1984. "The Simultaneous Measurement of Thermal Conductivity, Thermal Diffusivity, and Perfusion in Small Volumes of Tissue." *Journal of Biomechanical Engineering* 106 (August 1984): 192–97. doi:10.1115/1.3138482.
- Warmuth, Carsten, Stefan Nagel, Oliver Hegemann, Waldemar Wlodarczyk, and Lutz Lüdemann. 2007. "Accuracy of Blood Flow Values Determined by Arterial Spin Labeling: A Validation Study in Isolated Porcine Kidneys." *Journal of Magnetic Resonance Imaging : JMRI* 26 (2): 353–58. doi:10.1002/jmri.21011.
- Watson, C J E, and J H Dark. 2012. "Organ Transplantation: Historical Perspective and Current Practice." *British Journal of Anaesthesia* 108 Suppl (January): i29–42. doi:10.1093/bja/aer384.
- Wiig, Helge, Knut Aukland, Olav Tenstad, and Olav Tenstad Isola-. 2003. "Three-Dimensional Imaging of Vasculature and Parenchyma in Intact Rodent Organs with X-Ray Micro-CT." *Am J Physiol Heart Circ Physiol* 284: H416–24.
- Yuan, Xiaodong, Ashok J Theruvath, Xupeng Ge, Bernhard Floerchinger, Anke Jurisch, Guillermo García-Cardena, and Stefan G Tullius. 2010. "Machine Perfusion or Cold Storage in Organ Transplantation: Indication, Mechanisms, and Future Perspectives." *Transplant International :*

Official Journal of the European Society for Organ Transplantation 23 (6): 561–70.

doi:10.1111/j.1432-2277.2009.01047.x.

Chapter 3 – The Development of a Thin-Filmed, Non-Invasive Tissue Perfusion Sensor to Quantify Pressure Ischemia of Explanted Organs

Timothy O'Brien¹, Ali Roghanizad¹, John Robertson^{1, 2}, Thomas Diller¹

[1] Virginia Tech Mechanical Engineering

[2] Virginia Tech-Wake Forest School of Biomedical Engineering and Science

3.1 Abstract

A new thin-filmed perfusion sensor was developed using a heat flux gage, thin-film thermocouple, and a heating element. This sensor, the CHFT+, is an enhancement of the previously established CHFT sensor technology predominately used to quantify the severity of burns. The CHFT+ sensor was uniquely designed to improve tissue perfusion measurements on explanted organs, such as a porcine kidney. Due to the thin and semi-flexible nature of the new CHFT+ sensor assembly, perfusion measurements can be made from the underside of the organ resulting in a quantitative measure of pressure ischemia. Although, progress has been made in the development of machine perfusion devices, no system has yet considered the effect pressure ischemia could have on an explanted organ sitting on a dense surface. This sensor could potentially change the way organs preservation systems are designed, pushing biomedical and mechanical engineers towards designing an anatomical cassette or other pressure relieving technologies. Results from a live tissue test demonstrated, for the first time, the effects of pressure ischemia on an explanted porcine kidney.

Keywords Perfusion, Heat Flux, Temperature, Thin-Filmed, Non-Invasive, Pressure Ischemia

3.2 Introduction

According to the Organ Procurement and Transplant Network (OPTN), there are approximately 123,206 people in need of a life-saving organ transplant. Last year, a total of 27,036 transplants were performed. While the demand for organs increases every year, the consistent shortage in supply is disconcerting. The organ supply deficit can be attributed to several factors including insufficient donation to meet the needs, discarding of organs prior to transplantation due to concerns over quality, inability to transplant in a timely manner, and problems occurring during surgery. Figure 1 illustrates this grave problem in organ transplantation.

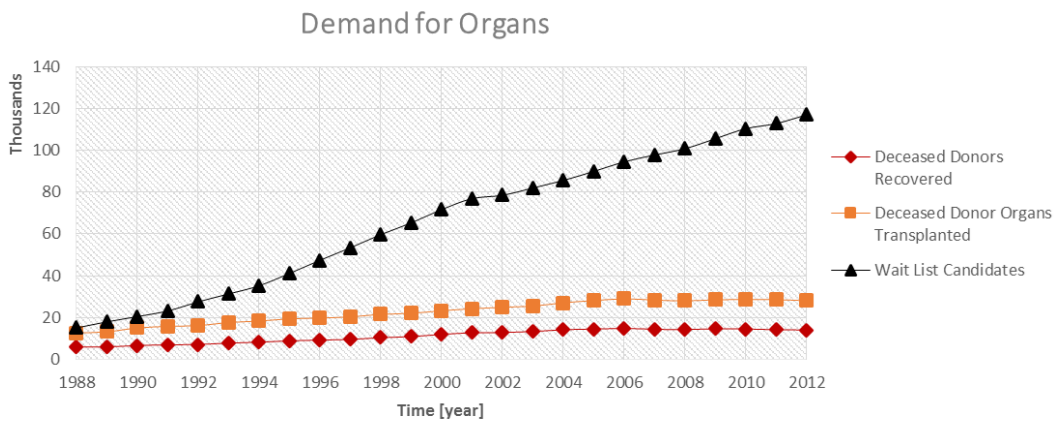


Figure 17. Demand for Organs

While improvements in organ preservation technology have developed immensely since the first successful kidney transplant performed by Dr. Joseph Murray in 1954, static cold storage (SCS) continues to be the “gold standard” of organ preservation. Although this simple, low-cost method has provided a workable technology over the years, it is hardly ideal. Most organs only survive a few hours

when outside the body in SCS. This method does not provide real-time monitoring or sensing to predict the organ vital health, forcing transplant surgeons to rely on the organ's physical appearance, a small biopsy, and consideration of the donor and recipient characteristics.

The development of machine perfusion organ preservation systems (hypothermic machine perfusion and normothermic machine perfusion) has affected the future of organ preservation, yet many of these systems are still overlooking one key feature, pressure ischemia. Pressure ischemia is simply the restriction of blood flow to tissue due to some applied pressure. The study of pressure ischemia becomes critical to the transport of explanted organs when considering the manner of which said organ is resting throughout the transition. Until now, pressure ischemia has been overlooked and underappreciated by most organ preservation systems.

In the work reported here, a novel, non-invasive, thin-filmed sensor was designed for measuring tissue perfusion on the underside of an explanted organ. Here, Smart Perfusion's Vasowave™ (VW) was utilized as the platform to support organ viability and collect vital data of explanted organs. During preservation, localized perfusion was measured on both the top side and underside of an explanted organ. The goal of this effort was to illustrate the need for future organ preservation systems to consider the effects of pressure ischemia during preservation.

3.3 Existing Perfusion Measurement Technologies

Tissue perfusion technology can be structured into two modes of technology, namely deep tissue and surface measurement. Magnetic Resonance Imaging (MRI), Positron Emission Tomography (PET), Single-Photon Emission Computer Tomography (SPECT), Micro Computer Tomography (MicroCT) and Thermal Diffusion Probe (TDP) are all methods defined with the deep tissue measurement mode. Laser Doppler Flowmetry (LDF), Laser Doppler Imaging (LDI), Doppler

Ultrasound (DU), and IR Thermal mapping all technologies collectively identified as tissue perfusion systems utilizing a surface measurement mode.

3.3.1 In-Depth Tissue Perfusion Methods

The measurement of deep tissue perfusion has is usually performed via a scan of the tissue region of interest followed by an image analysis. Some of these methods are more invasive than others, and may require a diffusible tracer to be added to the bloodstream/ perfusate stream in order to acquire meaningful results (Prinzen and Bassingthwaighte 2000). However, magnetic resonance imaging perfusion is non-invasive technology that has shown some success. Originally applied to measure the perfusion of a brain, MRI perfusion can be utilized on all types of tissue. Arterial Spin Labeling (ASL), the more common method of MRI perfusion measurement, involves the observation of magnetically tagged red blood cells passing through the region of interest. The signal produced is directly related to the number of red blood cells passing through that volumetric space (Montet et al. 2003; Detre 2008; Warmuth et al. 2007).

Positron Emission tomography is a comparable technology that requires the introduction of a radioactive tracer to the blood supply. Generally, the tracer is partnered with a carrier, such as glucose, that will deliver the radioactive tracer to the tissue of interest. As the carrier starts to decay, positrons are emitted. Gamma rays are produced from the positron-electron collisions that occur and these gamma rays are sent to a computer for image construction (Boellaard et al. 2006; Schelbert 2000; Nuutila and Kalliokoski 2000). Similarly to PET, Single-Photon Emission Computer Tomography also requires the use of a radioactive substance to be emitted into the blood stream. However, this technology emits a single gamma ray, rather than a double gamma ray. As well, the radioactive tracers utilized for SPECT have a longer decay time (Petersson et al. 2004). MicroCT is another method that involves the injection

of a tracer into the bloodstream and observing its movement over time. The CT scanner takes 2-dimensional images at various depths of the tissue of interest. These images slices are then stacked and re-constructed into a 3-dimensional model of the tissue. The perfusion is then estimated based on the location of the tracer (Badea et al. 2008; Nett et al. 2010; Wiig et al. 2003).

A potentially valuable in-depth tissue perfusion measurement technology that does not require image processing involves the use of a thermal diffusion probe. Here this probe is directly inserted into the tissue of interest, where the probe then measures the heat transfer exchange between the tissue and blood. Perfusion is later calculated utilizing the transient solution of the thermal energy equation. While this method is much more invasive, it does provide meaningful quantitative feedback rather than relative data (Khot et al. 2005; Valvano, Allen, and Bowman 1984).

3.3.2 Surface Tissue Perfusion Methods

Laser Doppler Flowmetry (LDF) is a well-established technique that utilizes low power lasers to send light over the desired tissue region. First, a probe is placed on the surface of the tissue. Laser light is sent to the tissue, which mostly scatters upon contact with the tissue surface, however, some light is reflected back and collected. Then the emitted and returned light signals are compared to calculate the Doppler shift, which can be related to the velocity of red blood cells flowing through the tissue. The signal is recorded as blood perfusion units (BPU), a relative unit scale. (Oltean et al. 2005; Niwayama and Sanaka 2005; Monstrey et al. 2008; Svedman et al. 1998) Another surface perfusion measurement technology that was based off of LDF is known as Laser Doppler Imaging (LDI). This method is comprised off the same principles as LDF, however, it scans an entire region of interest in a step-wise fashion, which constructs an image. Again, the end result yields the relative unit scale of BPU. (Monstrey et al. 2008)

More recently, a thermal convective probe comprising of the combination of a thin heat flux sensor and thin-filmed thermocouple was developed at Virginia Tech. This probe, the CHFT perfusion probe, originally designed to provide quantitative feedback on the severity of burns has since been applied to measure the perfusion of both intact and explanted organs. The CHFT probe measure the heat flux response to an imposed convective thermal event at the surface of the specimen tissue. (Mudaliar, Ellis, Ricketts, Lanz, Lee, et al. 2008; Alkhwaji, Vick, and Diller 2012; Al-khwaji, Vick, and Diller 2015)

3.4 Methodology

3.4.1 Mathematical Model

Temperature regulation is a critical parameter for life. Blood flow is the body's instrument for transporting essential nutrients, oxygen, waste products, and temperature to and from internal organs. In 1948, Harry H. Pennes developed a mathematical relationship between arterial blood flow and tissue temperature. This model provides a simple, yet accurate portrayal of the bio-heat process of tissue and has since been used to model various biological tissues. Pennes bio-heat equation assumes homogenous tissue properties, uniform metabolic heat generation, and a proportionality between the convective heat transfer entering tissue and the venous flow leaving the tissue (Pennes 1948).

3.4.1.1 System Model

This work utilized the Pennes bio-heat equation to model the perfusion of the surface of an explanted porcine kidney. For this particular model, two additional assumptions were been made. Here,

we assumed one dimensionality into the tissue and neglected the effects of metabolic heat generation. The Pennes bio-heat equation reduces to the form illustrated in Equation 1, where ρ is the density, c is the heat capacitance, w is the perfusion, T is the temperature of the tissue, T_{core} is the core temperature, k is the thermal conductivity of the tissue, t is time, and x is the direction of the heat transfer (Alkhwaji, Vick, and Diller 2012).

$$(\rho c)_p \frac{\partial T}{\partial t} = k \frac{\partial^2 T}{\partial x^2} - (\rho c w)_b (T - T_{core}) \quad [4]$$

The measured sensor temperature profile is modeled as a series of steps as shown in Equation 2.

$$\theta_s(t) = \theta_s(0) + \sum_{n=1}^{Nmax} \Delta\theta_{s,n} \cdot H(t - t_n) \quad [5]$$

Where $\theta = (T - T_{core})$ and $H(t)$ is the step function. Equation 3 displays the bio-heat equation in terms of the variable $\theta(x, t) = T(x, t) - T_{core}$.

$$(\rho c)_p \frac{\partial \theta}{\partial t} = k \frac{\partial^2 \theta}{\partial x^2} - (\rho c w)_b \theta \quad [6]$$

This mathematical model requires both an initial and transient solution. Alkhwaji provides a full explanation of this model and its mathematical solutions (Alkhwaji, Vick, and Diller 2012).

3.4.1.2 Parameter Estimation

A parameter estimation routine is utilized to determine the thermal contact resistance between the sensor and the tissue surface, tissue perfusion, and the core temperature of the specimen. These three system parameters are determined from the measured heat flux and temperature data. This process is highly iterative and minimizes the sum of the squares of the residuals between the measured data and the analytically calculated solution. The optimal perfusion, contact resistance, and core temperature values are determined once the error is driven to a minimum. Figure 2 explains this minimization process via a simple schematic where the variable S represents the error, R'' symbolizes thermal contact resistance, and ω_b is perfusion. This parameter estimation routine varies the thermal contact resistance and tissue perfusion one at a time over finer and finer ranges until a sufficient resolution has been achieved (Alkhwaji, Vick, and Diller 2012).

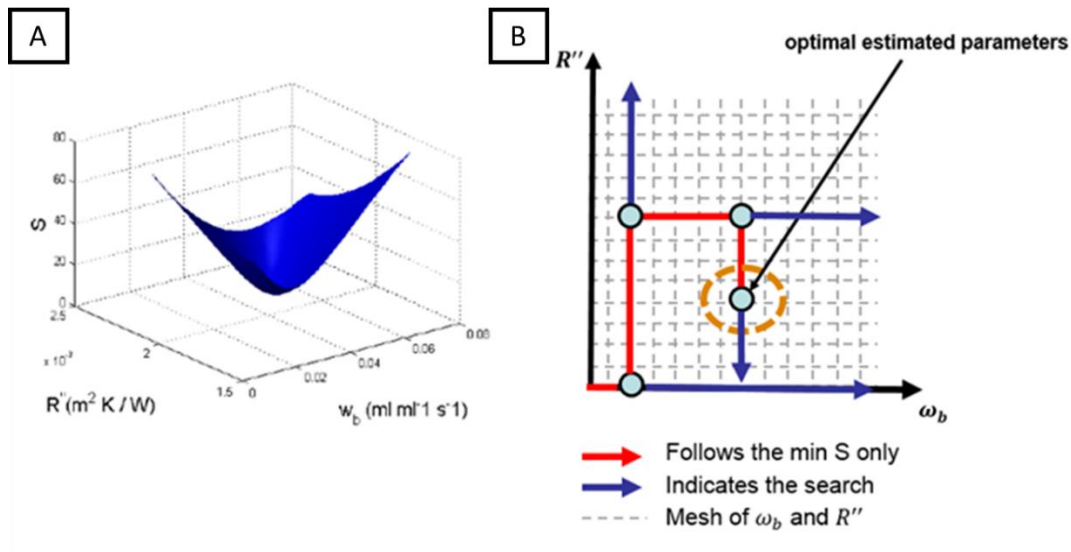


Figure 18. (A) Error Minimization. (B) Parameter Estimation Search Process Schematic

The core temperature, is initially calculated using the measured steady state values and recalculated for each new set of perfusion and contact resistance values using Equation 4.

$$T_{core} = T_{s,o} + \frac{q_{s,o}}{\left[\frac{k\sqrt{w_b/\alpha}}{1 + R'' k\sqrt{w_b/\alpha}} \right]} \quad [7]$$

3.4.2 Manufacturing of CHFT+ Sensor

The CHFT+ sensor is a combination of a thin heat flux sensor, thin temperature sensor, and thin heating element. The heat flux sensor is a thin film thermopile gage developed by RdF Corporation with a sensitivity of 18 mV (W/cm²). The 28.5-mm x 35.1-mm sensor has a thickness of 0.18-mm. The foil thermocouple was constructed with constantan and copper, resulting in a T-type thermocouple with 0.0127-mm thickness. This thermocouple was laminated to the front side of the heat-flux gage, while a MINCO Thin Polyimide Resistive Heater, with a diameter and thickness of 5.08-cm and 0.254-mm respectively, was laminated to the back side to establish a temperature difference for heat flux measurements. Figure 2 illustrates the individual sensors that were combined.

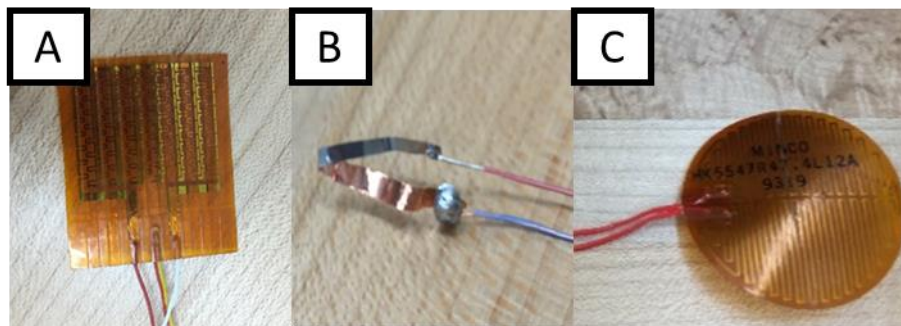


Figure 19. (A) Heat Flux Sensor (B) Foil Thermocouple (C) Resistive Heating Element

These sensors were stacked, as shown in Figure 3, with a thin (0.015-mm) layer of Mylar and thermally activated epoxy (John C. Doph Company, New Jersey) between each layer. The assembly was then placed within a HIX “Hobby Lite” heat press at 160°C for 3 hours.

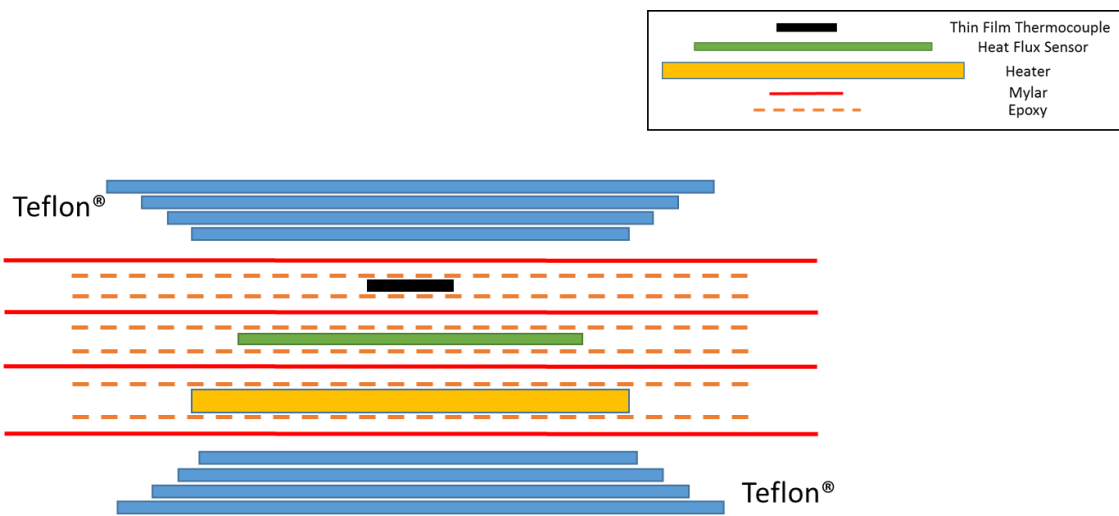


Figure 20. CHFT+ sensor layered assembly schematic

The sensor is 0.41-mm in thickness and its largest dimension stems from the heating element with a diameter of 50.8-mm. It is critical that the resistive heater is larger than the heat flux sensor and thermocouple in order to maintain 1-dimensional heat transfer into the tissue and agree with the mathematical model. The final product of the CHFT+ sensor is displayed in Figure 4.

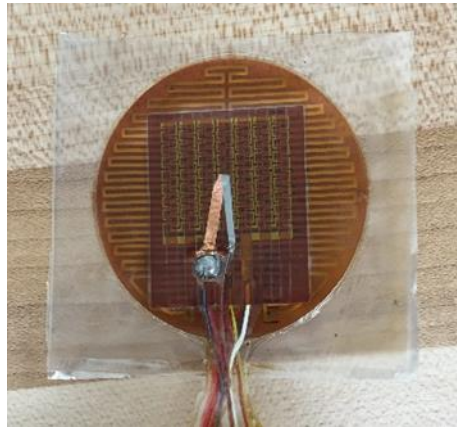


Figure 21. CHFT+ sensor

3.4.3 Controlled Phantom Tissue Testing

The CHFT+ sensor was extensively tested on a controlled phantom tissue testing system previously developed by Mudaliar et al. (Mudaliar, Ellis, Ricketts, Lanz, Scott, et al. 2008) This system essentially pumps temperature controlled water at a controlled rate through a small orifice and into a sponge. This sponge acts as the perfused tissue. Figure 5 shows this system in greater detail.

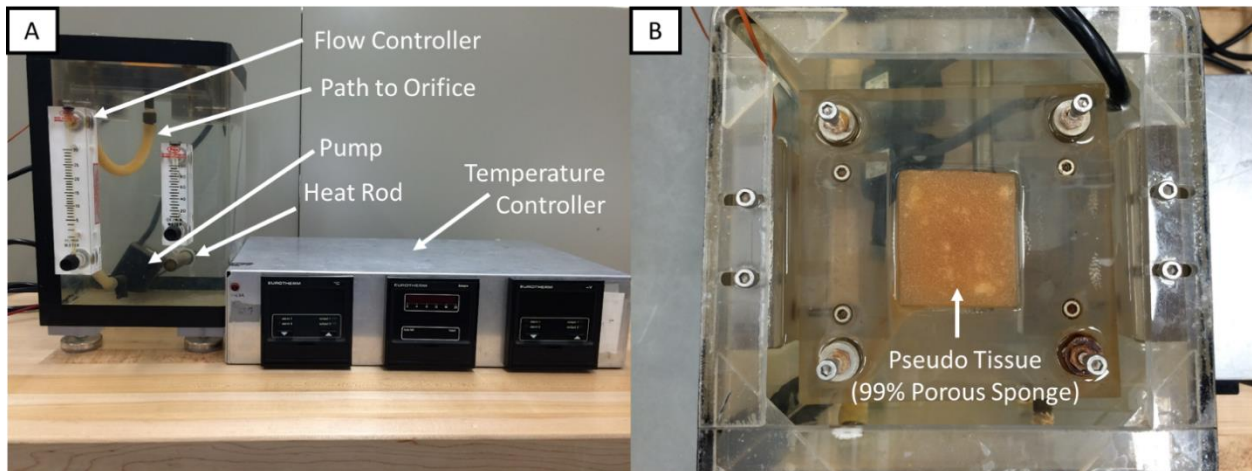


Figure 22. (A) Front view of the Phantom Perfusion System. (B) Top view displaying the sponge used on the Phantom Perfusion System

3.4.4 Explanted Porcine Kidney Testing

A porcine kidney was procured from a local abattoir, immediately fitted with Leur-Lock connectors and flushed at a constant pressure of ~90 mmHg with 1 liter of cold modified Phosphate Buffer Solution (PBS). During the initial flush interval, the porcine kidney was flipped on its alternate side every 250 mL to minimize the effects of pressure ischemia. Then, the organ was placed in a cooler of ice (Static Cold Storage) until anastomosed to Smart Perfusion LLC’s Vasowave™ (VW) organ preservation system at Virginia Tech. This organ preservation system is able to generate and monitor the response of any pulse or waveform, set and monitor the perfusate temperature, and monitor the fluid pH, dissolved oxygen content, conductivity, and flow rate. Figure 6 shows the current working research model of the Vasowave™, complete with a schematic illustrating the flow direction and a look at the cardio-emulating pressure waveform sent to the specimen.

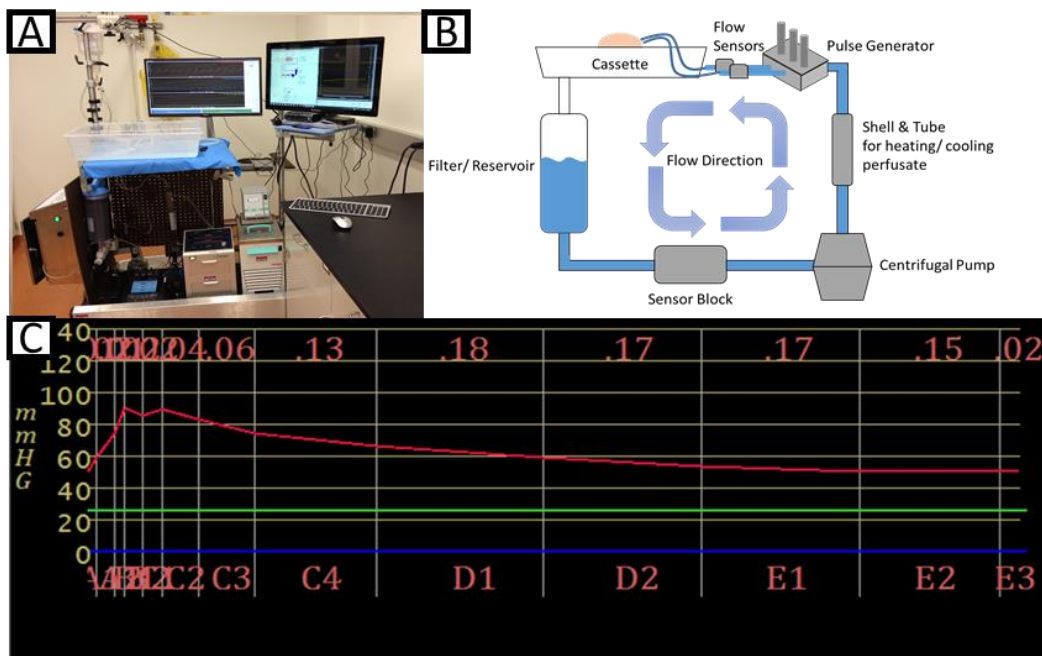


Figure 23. (A) Working Vasowave™ research model (B) Vasowave™ flow schematic (C) Cardio-emulating pressure waveform

For this test, a cardio-emulating physiologic pressure waveform of 90/50 mmHg was set and delivered to the organ, while the perfusate temperature was set to a sub-normothermic temperature of 20°C. The original CHFT sensor was used to measure perfusion on the top surface of the organ while the CHFT+ sensor was positioned beneath the organ to measure the perfusion of the vascular bed experiencing pressure ischemia. Figure 7 shows a schematic of the positioning of the CHFT+ sensor beneath a porcine kidney.

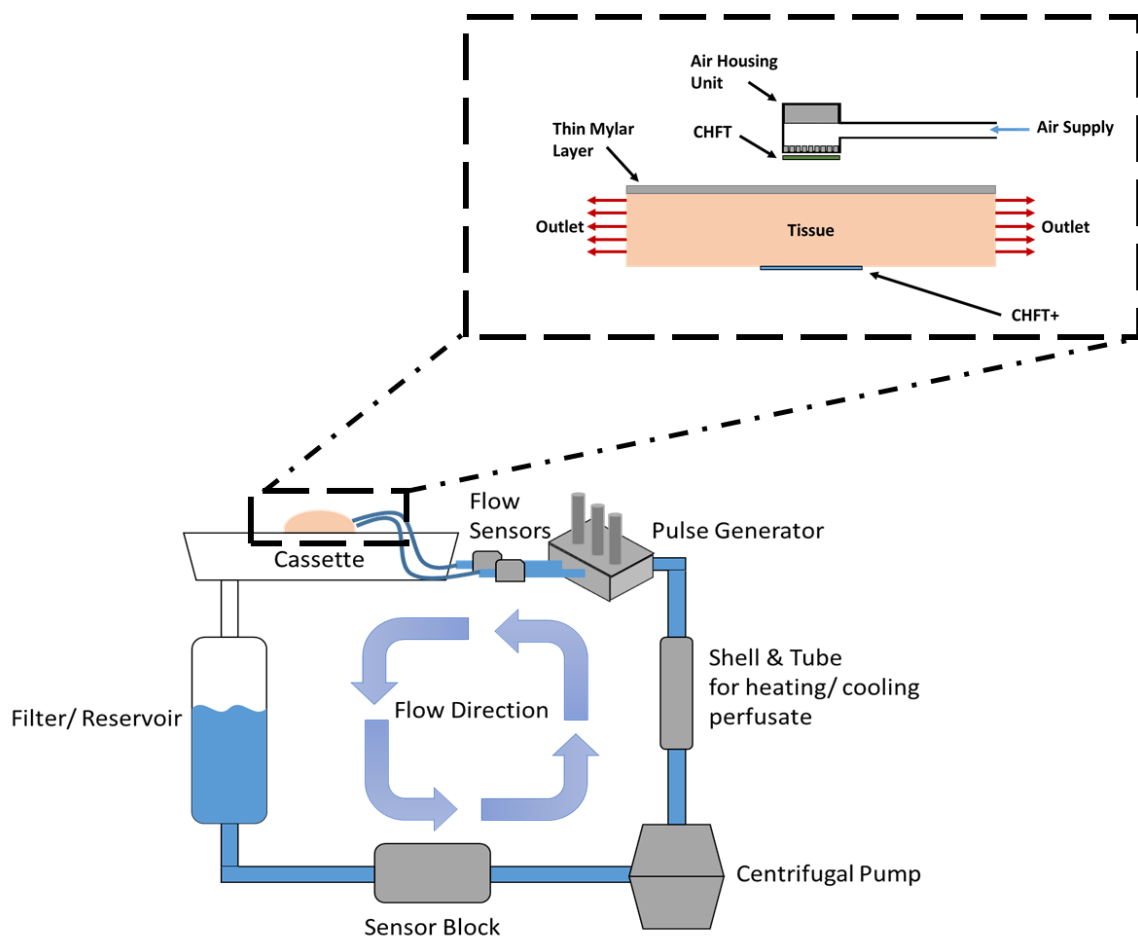


Figure 24. Schematic illustrating the positioning of the CHFT+ sensor beneath a porcine kidney within the VW organ preservation system.

3.5 Results & Discussion

3.5.1 Phantom Tissue Testing

The sensor was tested at 4 different flow rates (10 cm³/min – 25 cm³/min) at room temperatures (~25°C). The resulting heat flux and temperature curves were then plotted against one another and evaluated to determine the sensitivity of the sensor. Figure 8 shows the resulting heat flux and temperature curves.

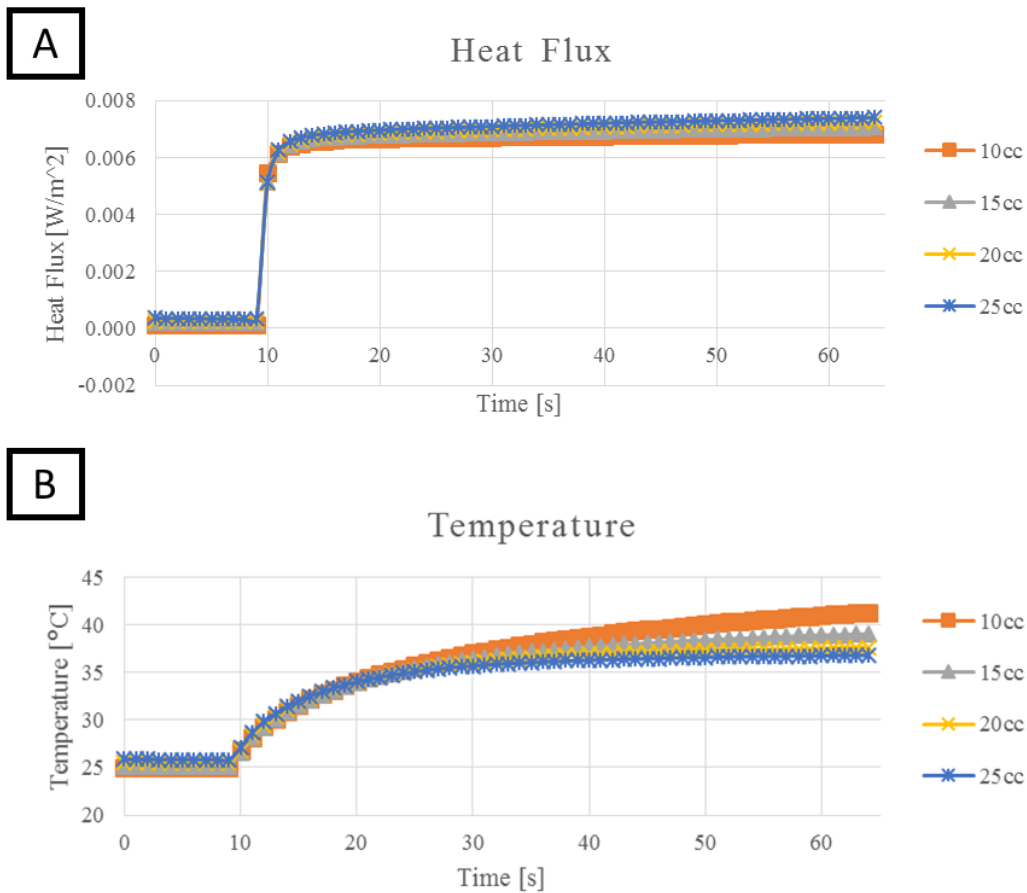


Figure 25. (A) Phantom Tissue Testing Heat Flux Curves (B) Phantom Tissue Testing Temperature Curves

The smooth curves indicate excellent contact with the pseudo tissue with zero disturbance from external sources. This is already a great improvement from the previously developed CHFT sensor, in which the user was required to continually hold the sensor to the tissue surface while maintaining a steady hand. Furthermore, there is a clear trend in flowrate and the measured heat flux and temperature curves. As the flow rate increases, the quicker the temperature curve reaches a steady state, and the larger the heat flux values rise.

This measured data was then run through the parameter estimation routine to search for the perfusion values. A sample of the values of the measured and analytical heat flux and temperature curves is shown in Figure 26. The measured and analytical curves match well.

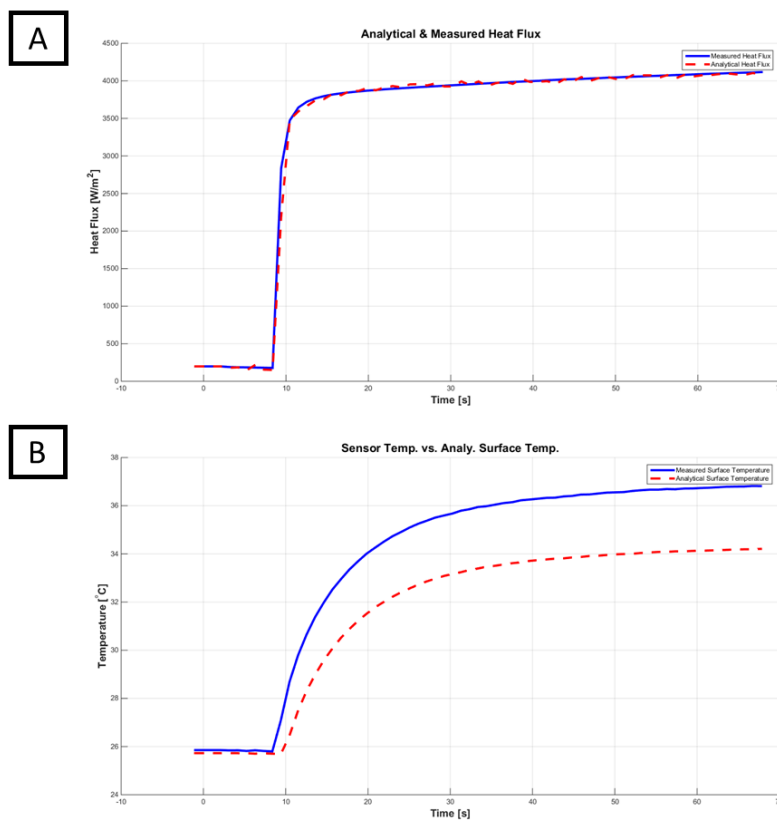


Figure 26. (A) Heat flux curve for 25 cm³/min (B) Temperature curve for 25 cm³/min

The results for each case are displayed in Table 3.1. The most critical information is illustrated in columns 1 and 3. As the set flow rate increases, the calculated tissue perfusion values also increase. This trend agreement indicates reasonable response of the system. The values of contact resistance and core temperature remain nearly the same, as expected in this controlled test.

Table 3. Phantom tissue perfusion results with CHFT+ sensor

Flow Rate [cm^3/min]	Contact Resistance [$m^2 k/w$]	Tissue Perfusion [ml/ml/s]	Core Temperature [$^{\circ}C$]	Error
10	0.000843	0.035939	24.67101	1.006647
15	0.00067048	0.05241693	24.7109036	0.3219636
20	0.000641	0.078535	25.06384	0.179402
25	0.000639	0.104209	25.29244	0.182768

These perfusion values were then compared to the Pennes model perfusion results from Mudaliar et al. (Mudaliar et al. 2007). The percentage difference between the perfusion values are different because the CHFT+ is a much larger sensor and the thermal event conditions are reasonably dissimilar. Table 3 shows this comparison in greater detail.

Table 4. Comparison of CHFT+ perfusion and the Pennes model from Mudaliar et al.

Flow Rate [cm^3/min]	CHFT+ Perfusion [ml/ml/s]	Pennes Perfusion [ml/ml/s]	Percentage Difference [%]
10	0.035939	0.0186	63.58385742
15	0.05241693	0.0333	44.60479394
20	0.078535	0.0491	46.12371215
25	0.104209	0.0658	45.18466669

3.5.2 Live Tissue Testing

It was hypothesized that the vasculature on the underside of the explanted organ would experience lower perfusion due to the pressure exerted by the dense surface the organ is resting on. Figure 27 shows the perfusion comparison between the topside of the organ (measured with the CHFT sensor), and the underside of the organ (measured with the CHFT+ sensor). There was some fluctuation throughout the course of the experiment. However, the perfusion of the vasculature on the underside of the organ was lower than the topside for the majority of the 12 hr. experiment. More repetitions of these experiments should be performed to confirm these results.

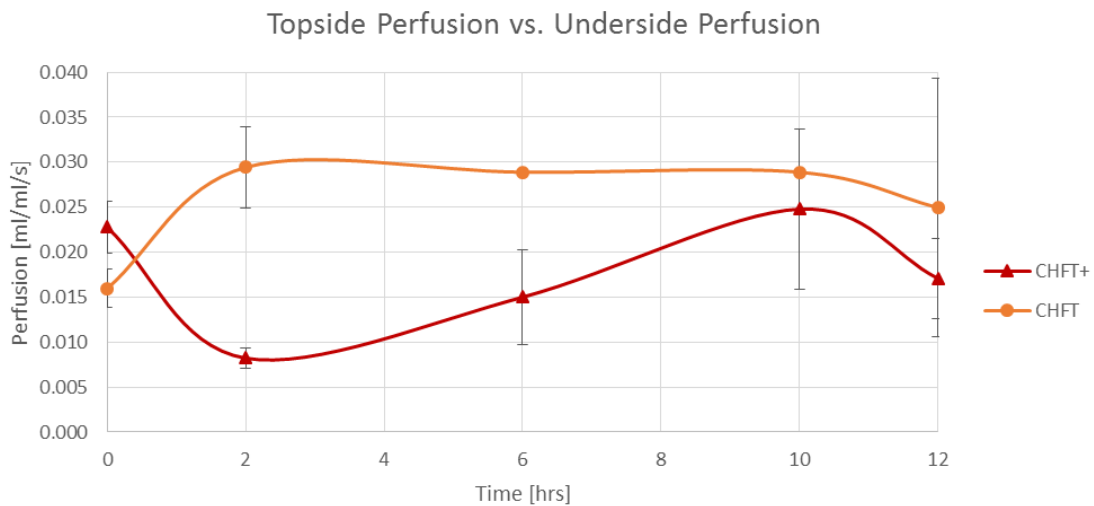


Figure 27. Comparison of perfusion on the topside against the underside

The CHFT and CHFT+ core temperature estimates were evaluated and compared against the venous fluid temperature. Figure 28 shows the resulting temperature comparison over the course of the 12-hr experiment.

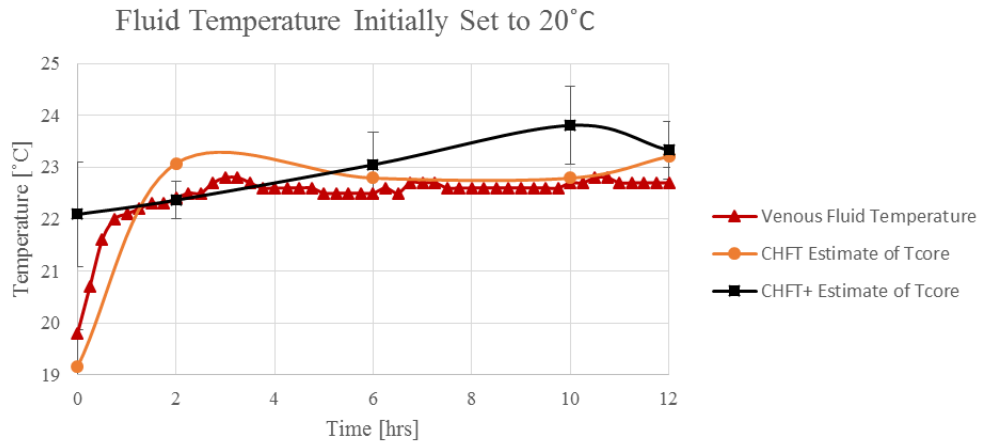


Figure 28. (A) Infrared image of porcine kidney. (B, C) Image processing program output.

The CHFT and CHFT+ sensor estimates for core temperature were both no more than 1°C off from the measured fluid temperature, suggesting a good estimation for both sensors.

3.6 Conclusion

This work illustrated the manufacture of a novel perfusion sensing technology and exploited its unique qualities to measure and evaluate the perfusion of an explanted porcine kidney from its underside for the first time. The performance of the CHFT+ sensor was effectively shown in a controlled phantom tissue setting, where the sensor displayed good repeatability and sensitivity.

Live tissue testing was acquired from the application of the CHFT+ sensor on an explanted porcine kidney. Preliminary results indicate that the perfusion on the underside of an explanted organ could be hindered by the occurrence of pressure ischemia. Although more testing needs to be performed to verify these results, the implication that the perfusion on the underside of an explanted organ is lesser

than that of the topside is substantial and could effectively change the way the organ preservation technologies are designed.

In order to statistically demonstrate the impact pressure ischemia has on explanted organs, more studies should be performed. Furthermore, organs procured, flushed and immediately placed on the Vasowave™ organ preservation system, rather than approximately 2 hours of cold ischemia between the initial flush and anastomosed to the Vasowave could lead to better results. As well, a commercially available perfusate, such as a Belzer UW solution, should be used for organs preserved at sub-normothermic temperatures.

3.7 References

- Alkhwaji, Abdusalam, Brian Vick, and Tom Diller. 2012. "New Mathematical Model to Estimate Tissue Blood Perfusion, Thermal Contact Resistance and Core Temperature." *Journal of Biomechanical Engineering* 134 (8): 081004. doi:10.1115/1.4007093.
- Al-khwaji, Abdusalam, Brian Vick, and Tom Diller. 2015. "Modeling and Estimating Simulated Burn Depth Using the Perfusion and Thermal Resistance Probe" 7 (September 2013): 1–9. doi:10.1115/1.4024160.
- Badea, C T, M Drangova, D W Holdsworth, and G a Johnson. 2008. "In Vivo Small-Animal Imaging Using Micro-CT and Digital Subtraction Angiography." *Physics in Medicine and Biology* 53: R319–50. doi:10.1088/0031-9155/53/19/R01.
- Boellaard, Ronald, Paul Knaapen, Abraham Rijbroek, Gert J J Luurtsema, and Adriaan a. Lammertsma. 2006. "Evaluation of Basis Function and Linear Least Squares Methods for Generating Parametric Blood Flow Images Using ¹⁵O-Water and Positron Emission Tomography." *Molecular Imaging and Biology* 7 (August): 273–85. doi:10.1007/s11307-005-0007-2.
- Cannon, Robert M., Guy N. Brock, R. Neal Garrison, Jason W. Smith, Michael R. Marvin, and Glen a. Franklin. 2013. "To Pump or Not to Pump: A Comparison of Machine Perfusion vs Cold Storage for Deceased Donor Kidney Transplantation." *Journal of the American College of Surgeons* 216 (4). Elsevier Inc: 625–34. doi:10.1016/j.jamcollsurg.2012.12.025.
- Detre, Ja - Google. 2008. "Traduzido - Arterial Spin Labeled Perfusion Mri." *Clinical Neurology*, 6–12. http://usa.healthcare.siemens.com/siemens_hwem-hwem_sxxa_websites-context-root/wcm/idc/groups/public/@us/@clinicalspec/documents/download/mdaw/nde3/~edisp/magneto_m_mr-clinical-cases-asl-case-00305305.pdf.

- Gallinat, Anja, Cyril Moers, Jürgen Treckmann, Jacqueline M. Smits, Henry G D Leuvenink, Rolf Lefering, Ernest Van Heurn, et al. 2012. “Machine Perfusion versus Cold Storage for the Preservation of Kidneys from Donors ≥ 65 Years Allocated in the Eurotransplant Senior Programme.” *Nephrology Dialysis Transplantation* 27 (July): 4458–63. doi:10.1093/ndt/gfs321.
- Khot, Monica B, Peter K M Maitz, Benjamin R Phillips, H Frederick Bowman, Julian J Pribaz, and Dennis P Orgill. 2005. “Thermal Diffusion Probe Analysis of Perfusion Changes in Vascular Occlusions of Rabbit Pedicle Flaps.” *Plastic and Reconstructive Surgery* 115: 1103–9. doi:10.1097/01.PRS.0000156546.45229.84.
- Majchrzak, Ewa. “3d Thermal Wave Model of Bioheat Transfer - Solution by Means of Finite Difference Method,” no. 2.
- Moers, Cyril et al. 2009. “New England Journal.” *The New England Journal of Medicine*, 1495–1504.
- Monstrey, Stan, Henk Hoeksema, Jos Verbelen, Ali Pirayesh, and Phillip Blondeel. 2008. “Assessment of Burn Depth and Burn Wound Healing Potential.” *Burns* 34: 761–69. doi:10.1016/j.burns.2008.01.009.
- Montet, Xavier, Marko K Ivancevic, Jacques Belenger, Manuel Jorge-Costa, Sybille Pochon, Antoinette Pechère, François Terrier, and Jean-Paul Vallée. 2003. “Noninvasive Measurement of Absolute Renal Perfusion by Contrast Medium-Enhanced Magnetic Resonance Imaging.” *Investigative Radiology* 38 (9): 584–92. doi:10.1097/01.RLI.0000077127.11949.8c.
- Mudaliar, Ashvinikumar V, Thomas E Diller, D Sc, Elaine P Scott, Ph D Co-chair, Otto I Lanz, Diplomate Acvs, Danesh Tafti, D Ph, and Brian Vick. 2007. “Development of a Phantom Tissue for Blood Perfusion Measurement and Noninvasive Blood Perfusion Estimation in Living Tissue Virginia Polytechnic Institute and State University in Partial Fulfillment of the Requirements for the Degree of Doctor of Philosop.”

- Mudaliar, Ashvinikumar V, Brent E Ellis, Patricia L Ricketts, Otto I Lanz, Charles Y Lee, Thomas E Diller, and Elaine P Scott. 2008. "Noninvasive Blood Perfusion Measurements of an Isolated Rat Liver and an Anesthetized Rat Kidney." *Journal of Biomechanical Engineering* 130 (6): 061013. doi:10.1115/1.2978989.
- Mudaliar, Ashvinikumar V, Brent E Ellis, Patricia L Ricketts, Otto I Lanz, Elaine P Scott, and Thomas E Diller. 2008. "A Phantom Tissue System for the Calibration of Perfusion Measurements." *Journal of Biomechanical Engineering* 130 (October 2008): 051002. doi:10.1115/1.2948417.
- Nett, Brian E, Robert Brauweiler, Willi Kalender, Howard Rowley, and Guang-Hong Chen. 2010. "Perfusion Measurements by Micro-CT Using Prior Image Constrained Compressed Sensing (PICCS): Initial Phantom Results." *Physics in Medicine and Biology* 55: 2333–50. doi:10.1088/0031-9155/55/8/014.
- Niwayama, Jun, and Tsutomu Sanaka. 2005. "Development of a New Method for Monitoring Blood Purification: The Blood Flow Analysis of the Head and Foot by Laser Doppler Blood Flowmeter during Hemodialysis." *Hemodialysis International. International Symposium on Home Hemodialysis* 9: 56–62.
- Nuutila, P, and K Kalliokoski. 2000. "Use of Positron Emission Tomography in the Assessment of Skeletal Muscle and Tendon Metabolism and Perfusion." *Scandinavian Journal of Medicine & Science in Sports* 10: 346–50.
- Oltean, M, a Aneman, G Dindelegan, J Mólne, M Olausson, and G Herlenius. 2005. "Monitoring of the Intestinal Mucosal Perfusion Using Laser Doppler Flowmetry after Multivisceral Transplantation." *Transplantation Proceedings* 37 (8): 3323–24. doi:10.1016/j.transproceed.2005.09.032.

- Orlando, Giuseppe, Christopher Booth, Zhan Wang, Giorgia Totonelli, Christina L. Ross, Emma Moran, Marcus Salvatori, et al. 2013. "Discarded Human Kidneys as a Source of ECM Scaffold for Kidney Regeneration Technologies." *Biomaterials* 34 (24). Elsevier Ltd: 5915–25. doi:10.1016/j.biomaterials.2013.04.033.
- Patel, S K, O G Pankewycz, N D Nader, M Zachariah, R Kohli, and M R Laftavi. 2012. "Prognostic Utility of Hypothermic Machine Perfusion in Deceased Donor Renal Transplantation." *Transplantation Proceedings* 44 (7). Elsevier Inc.: 2207–12. doi:10.1016/j.transproceed.2012.07.129.
- Pennes, Hh. 1948. "Analysis of Tissue and Arterial Blood Temperatures in the Resting Human Forearm." *Journal of Applied Physiology*, 5–34. doi:9714612.
- Petersson, Johan, Alejandro Sánchez-Crespo, Malin Rohdin, Stéphanie Montmerle, Sven Nyrén, Hans Jacobsson, Stig a Larsson, et al. 2004. "Physiological Evaluation of a New Quantitative SPECT Method Measuring Regional Ventilation and Perfusion." *Journal of Applied Physiology (Bethesda, Md. : 1985)* 96 (November 2003): 1127–36. doi:10.1152/jappphysiol.00092.2003.
- Prinzen, Frits W., and James B. Bassingthwaite. 2000. "Blood Flow Distributions by Microsphere Deposition Methods." *Cardiovascular Research* 45: 13–21. doi:10.1016/S0008-6363(99)00252-7.
- Schelbert, Heinrich R. 2000. "PET Contributions to Understanding Normal and Abnormal Cardiac Perfusion and Metabolism." *Annals of Biomedical Engineering* 28: 922–29. doi:10.1114/1.1310216.
- Svedman, Cecilia, George W. Cherry, Elizabeth Strigini, and Terence J. Ryan. 1998. "Laser Doppler Imaging of Skin Microcirculation." *Acta Dermato-Venereologica* 78: 114–18. doi:10.1080/000155598433430.

- Treckmann, Jürgen, Manfred Nagelschmidt, Thomas Minor, Fuat Saner, Stefano Saad, and Andreas Paul. 2009. "Function and Quality of Kidneys after Cold Storage, Machine Perfusion, or Retrograde Oxygen Persufflation: Results from a Porcine Autotransplantation Model." *Cryobiology* 59 (1). Elsevier Inc.: 19–23. doi:10.1016/j.cryobiol.2009.03.004.
- Valero, R, C Cabrer, F Oppenheimer, E Trias, J Sánchez-Ibáñez, F M De Cabo, a Navarro, et al. 2000. "Normothermic Recirculation Reduces Primary Graft Dysfunction of Kidneys Obtained from Non-Heart-Beating Donors." *Transplant International : Official Journal of the European Society for Organ Transplantation* 13 (4): 303–10.
- Valvano, J W, J T Allen, and H F Bowman. 1984. "The Simultaneous Measurement of Thermal Conductivity, Thermal Diffusivity, and Perfusion in Small Volumes of Tissue." *Journal of Biomechanical Engineering* 106 (August 1984): 192–97. doi:10.1115/1.3138482.
- Warmuth, Carsten, Stefan Nagel, Oliver Hegemann, Waldemar Wlodarczyk, and Lutz Lüdemann. 2007. "Accuracy of Blood Flow Values Determined by Arterial Spin Labeling: A Validation Study in Isolated Porcine Kidneys." *Journal of Magnetic Resonance Imaging : JMRI* 26 (2): 353–58. doi:10.1002/jmri.21011.
- Watson, C J E, and J H Dark. 2012. "Organ Transplantation: Historical Perspective and Current Practice." *British Journal of Anaesthesia* 108 Suppl (January): i29–42. doi:10.1093/bja/aer384.
- Wiig, Helge, Knut Aukland, Olav Tenstad, and Olav Tenstad Isola-. 2003. "Three-Dimensional Imaging of Vasculature and Parenchyma in Intact Rodent Organs with X-Ray Micro-CT." *Am J Physiol Heart Circ Physiol* 284: H416–24.
- Yuan, Xiaodong, Ashok J Theruvath, Xupeng Ge, Bernhard Floerchinger, Anke Jurisch, Guillermo García-Cardena, and Stefan G Tullius. 2010. "Machine Perfusion or Cold Storage in Organ Transplantation: Indication, Mechanisms, and Future Perspectives." *Transplant International :*

Official Journal of the European Society for Organ Transplantation 23 (6): 561–70.

doi:10.1111/j.1432-2277.2009.01047.x.

Chapter 4 – Conclusions and Recommendations

4.1 – Conclusions

In the work reported here, the use of a non-invasive perfusion sensor was applied to explanted porcine kidneys to investigate the effect of perfusate temperature on organ vascular health. The combined heat flux and temperature (CHFT) sensor delivered repeatable perfusion information in both a controlled phantom tissue testing environment, as well as on live porcine tissue. Results indicated that while the organ vasculature experienced vasodilation for the higher temperatures, the tissue also degraded much more significantly over time. Furthermore, the design and manufacture of a novel perfusion sensing technology was reported. This thin, semi-flexible CHFT+ sensor is an enhancement to the previously developed CHFT sensor from Virginia Tech. The performance of the CHFT+ sensor was effectively shown in a controlled phantom tissue setting, where the sensor displayed good repeatability and sensitivity. This novel technology enabled the measurement and evaluation of perfusion from the underside of an explanted kidney was investigated for the first time. Preliminary results suggest that pressure ischemia could be disrupting the flow at the capillary level.

Overall, understanding the effect of temperature and pressure ischemia on explanted organs could lead to longer preservation periods, invention of pressure relieving technologies for explanted organs, as well as improving post-transplant graft survival.

4.2 – Recommendations

A much wider range of perfusate temperatures should be explored to better identify the optimal preservation temperature. Also, organs should be procured in-house and immediately placed on the Vasowave™ organ preservation system at the desired perfusate temperature. More studies should be carried out to statistically verify the effects of pressure ischemia on perfusion. Lastly, a commercially available perfusate, such as a Belzer UW solution, should be used for organs preserved at sub-normothermic temperatures and another oxygen carrying solution for the higher temperature experiments. It is critical to ensure that the explanted tissue is provided all the nutrients vital to that specific temperature range.

Appendices

Appendix A – MATLAB CODE (Parameter Estimation Routine)

This program was designed to load measured heat flux and temperature data, organize it appropriately, and send it through a parameter estimation routine. The parameter estimation routine iteratively searches for the best perfusion and thermal contact resistance values that minimize the error in the analytical solution. Then, the program plots the measured and analytical curves for both the surface temperature and heat flux.

```
%% *****
% Transient Bioheat Equation
%
% This program was designed to estimate the blood perfusion of tissue for
% the quantification of burn wounds, organ perfusion, and many other
% applications
%
% code developed by Abdusalam Alkhwaji
% code modified by Tim O'Brien
%*****

%% Clear workspace, close windows, and clear the command window
close all;
clear all;
clc;
format long e;

%% Load data from LabView and store to the variable y
load t_4.lvm;
y = t_4;

%% Set Constants
maximum = 31;
iteration = 10;
maximum2 = 31;
ratio = 15;
oo_max = 5;

%% Domain for blood perfusion and contact resistances
% Blood perfusion
W_min = 0.00000000000000011111;
W_max = 0.11111111111111111111;
```

```

factor1 = 0;    %avoids zooming to the negative direction

%% Calibration's factors
% Making sure that the heat flux sign is in the right direction
if y(2,2)>0
    SignHF = 1;
else SignHF = -1;
end

% If the core temperature of the tissue is below room temperature (~25C),
% multiply the Calibration_HF by a negative 1.
Constant = 10000000;
Calibration_HF = SignHF*18;    %[18 mV/W/cm^2]
% Calibration_HF = SignHF*2.1;    %[2.1 mV/W/cm^2]

%% Time Instances
start = 1;    % begin steady state probelm
start1 = 5; % begin transient problem
nmax = length(y(start:end,1));    %Total number of samples
stop = nmax;    %Total Time [s]

%% Constant to stop at the initial temperature measurement
if start1 > 1
    stop1 = 1;
else
    stop1 = 0;
end

```

```

%% Average of the initial measured temperature
Tii = y(1:start1-stop1,3);
Ti = mean(Tii);

%% Average of the initial measured heat flux
QmOff = (10000000/Calibration_HF)*y(1:start1-stop1,2);
Qmi = mean(QmOff);

%% Make sure the output of the thermocouple and heat flux sensor is stable
Qm = (Constant/Calibration_HF)*y(start:stop,2); % Heat Flux

%% Measured Heat flux and Temperature Data
t = y(start:stop,1)-start; % Delta_t
T0 = y(start:stop,3); % Surface Temperature
i = 1:start1-stop1; % Counter
T0(i) = Ti; % makes the first start:stop values == avg. measured temp.
Qm(i) = Qmi; % makes the first start:stop values == avg. measured HF

%% Human Kidney (Cortex) Tissue Properties
ro = 1049; % Density of tissue kg/m^3
cb = 3587; % Specific heat of tissue J-kg/k
k = 0.53; % Thermal conductivity of tissue W/m-k

%% Starting Parameter Estimation Routine

GSDOR=1000; % initial global minimum error

```

```

%% Zoom & Iterate around the optimal values of wbj (perfusion)
% and Rthi (thermal resistance) by "nmn" iterations
wbmin = W_min; % set minimum perfusion value
Rthmin = R_min; % set minimum thermal resistance value

]for nmn = 1:iteration % iteration for optimization routine

    % elm_line3 function
    Rth_range = elm_line3 (R_min,R_max,maximum,ratio); % function call for elm_line3
    wb_range = elm_line3 (W_min,W_max,maximum,ratio); % function call for elm_line3

    length_wb = (W_max-W_min)/maximum;
    length_Rth = (R_max-R_min)/maximum;

    jjj=1;
    oo=1;

] while (jjj<maximum+1 && oo < oo_max) %start_Rth < maximum && start_wb < maximum

    if mod(oo,2) == 0 % wb=wbmin --> wbmax
        nnRth = 0;
        nnwb = 1;
        Rth = Rth_range(jjj);
        wb = wbmin;
        if jjj == maximum
            oo = oo+1;
            jjj = 1;
            Rth = Rthmin;
        end
    else
        nnRth = 1;
        nnwb = 0;
    end
end

```



```

%% LOOKING FOR THE MINIMUM ERROR
% Summation of the square-root of the errors for each wbj, Rthi and iteration value "nmn"

errTRth(jjj) = SDOR;

if (nmn==1 && oo==1 && jjj==1)
    GSDOR = SDOR;
end

wbb(jjj,oo,nmn) = wb;
Rthh(jjj,oo,nmn) = Rth;
errTRthh(jjj,oo,nmn) = errTRth(jjj);

if errTRth(jjj) < GSDOR

    if nnwb == 1
        Rthmin = Rth; % Minimum Contact Resistance
        wbmin = wb; % Minimum Blood perfusion
        Ta0_opt = Ta0; % Optimal Tcore
    end

    if nnRth == 1
        Rthmin = Rth; % Minimum Contact Resistance
        wbmin = wb; % Minimum Blood perfusion
        Ta0_opt = Ta0; % Optimal Tcore
    end

    GSDOR = errTRth(jjj);
end

jjj = jjj+1;

```

```

Rth = Rthmin;
wb = wb_range(jjj);

if jjj == maximum
    oo = oo+1;
    jjj = 1;
    wb = wbmin;
end
end

```

```

% set variables
beta=wb;
alphaa=k/ro/cb;

```

```

%% Solving for wb, Rth and iteration value (nmn)

```

```

% Estimating the core temperature

```

```

Ta0=Ti-Qm1/(k*sqrt(beta/alphaa)/(1+Rth*k*sqrt(beta/alphaa)));

```

```

% Initial temperature at the skin u(x=0, t=0)

```

```

u(1,1)=(Ti-Ta0)*(1/(1+Rth*k*sqrt(beta/alphaa)));

```

```

% Calculating SDOR (global error)

```

```

[SDOR] = FuncStep_SDOR_v2(start1,u(1,1),T0,Ta0,t,beta,alphaa,k,Rth,ro,cb,nmax,Qm);

```

```

end
%% Meshing around the optimal solution
[R_min,R_max,W_min,W_max] = Meshing_PE(Rthmin,length_Rth,wbmin,length_wb, factor1, iteration);
maximum = maximum2;
end % End the N iteration

%% The optimal results are:
Rth = Rthmin;
wb = wbmin;
Ta0 = Ta0_opt;
GSDOR;
Results = [Rth, wb, Ta0, GSDOR];

%% Evaluating the optimal results within the mathematical model

% Constants for the new solution
alphaa = k/ro/cb;
beta = wb;

% steady state temperature solution:
u = (Ti-Ta0) * (1 / (1+Rth*k*sqrt(beta/alphaa)));

% Evaluating the analytical solution with optimal EP
[qAnaly, SkinTemp] = FuncStepAnaly(start1,u,T0,Ta0,t,beta,alphaa,k,Rth,ro,cb,nmax);

%% Plot Transient against Measured

%Plot of Temperature
figure(1);
PlotSolutionTemperature(nmax,Ta0,T0,SkinTemp,u,t);

%Plot of HeatFlux
figure(2);
PlotSolutionHF(nmax,qAnaly,t,Qm);

```

Appendix B – LabVIEW (Heat Flux and Temperature Measurement)

LabVIEW was used to record all experimental data. The front panel and block diagram are shown in Figure 28.

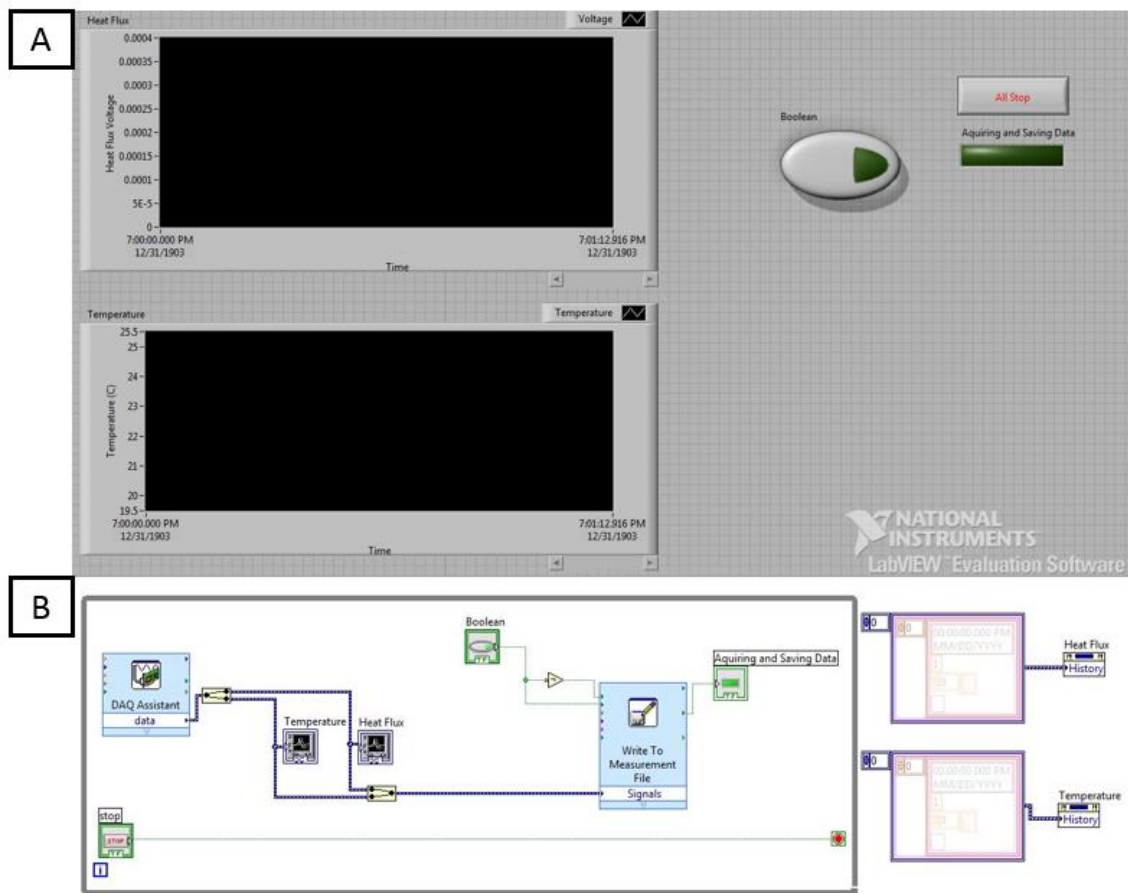


Figure 29. (A) Front Panel (B) Block Diagram

Appendix C – Instructions for Manufacturing the CHFT+ Sensor

A CHFT+ sensor is the combination of a heat flux sensor, thermocouple and heating pad. The heat flux sensor must have one side that is free of wire leads and wire connections. This insures that the heat flux sensor placed on the organ is smooth and without deformities. The heat flux sensor must also be as flexible as possible without undermining its structural integrity. This allows for better contact between the heat flux sensor and organ tissue. A simple resistivity test of the heat flux sensor using a multi-meter should insure that the heat flux sensor is operational and fully functional. Heat flux sensors are susceptible to a multitude of problems after increased use and time. A constant resistivity value insures proper function of the heat flux sensor before use. In addition to the resistivity test, it's important to determine and verify the heat flux sensor's sensitivity and accuracy before assembly. This will insure that the heat flux sensor is operating normally before it is used in the CHFT+. Calibration can be done using the R-MATIC heat flow meter. The value obtained from the R-MATIC testing, should be compared to the manufacture's specification. If the manufacture's specification is not available, the R-MATIC can be operated at a series of different temperature differences in order make sure of a constant and accurate sensitivity.

Since the thermocouple will be situated between the organ tissue and heat flux sensor, a thin film thermocouple must be used in order to insure full contact. It's important that full contact occurs between the two respective surfaces. Similar to the heat flux sensor, the thermocouple must be tested in order to insure proper function and accuracy before it is considered for CHFT+ development. The thin film thermocouple used in the CHFT+ sensor was made from constantan and copper. The two materials were been spot welded at their apex and have been designed so that the wire leads are close to each other upon exit from the CHFT+.

In order to facilitate and insure uniform heat flux, it is important that the resistive heater be larger than the heat flux sensor. This insures one dimensional heat transfer through the heat flux sensor which is required in order to agree with the mathematical model in place. The heater's resistance should be measured in order to insure proper function. Additionally, it may be of interest to calculate the specific watt density provided by the heater given an input voltage and heater resistance. The specific watt density can be used to estimate different design values given related thermal conductivity and heat capacity values. Figure 4 shows a resistive heater that would be suitable for use. Like the heat flux sensor, it's important that one side of the heater does not have any wire leads in order to insure full contact with heat flux sensor.

Each element above should be checked for nicks, cuts, scrapes or any other deformities that may cause an electrical short and otherwise compromise the CHFT+ long term functionality.

The following items are required for assembly:

- Acetone
- 4 pieces of Mylar (approximately 4x the size of the heating element)
- Thermally activated epoxy (John C. Dolph Company)
- Epoxy brush
- Teflon[®] (2 sets of 4 pieces that increase in size)
- Kapton[®] tape
- HIX "Hobby Lite" heat press

In order to successfully build this device, it's important to follow each step in order as outlined below. Any deviation from the predetermined steps may result in a misaligned and/or defective CHFT+. Figure 29 provides a schematic to visually aid the assembly of the CHFT+ sensor.

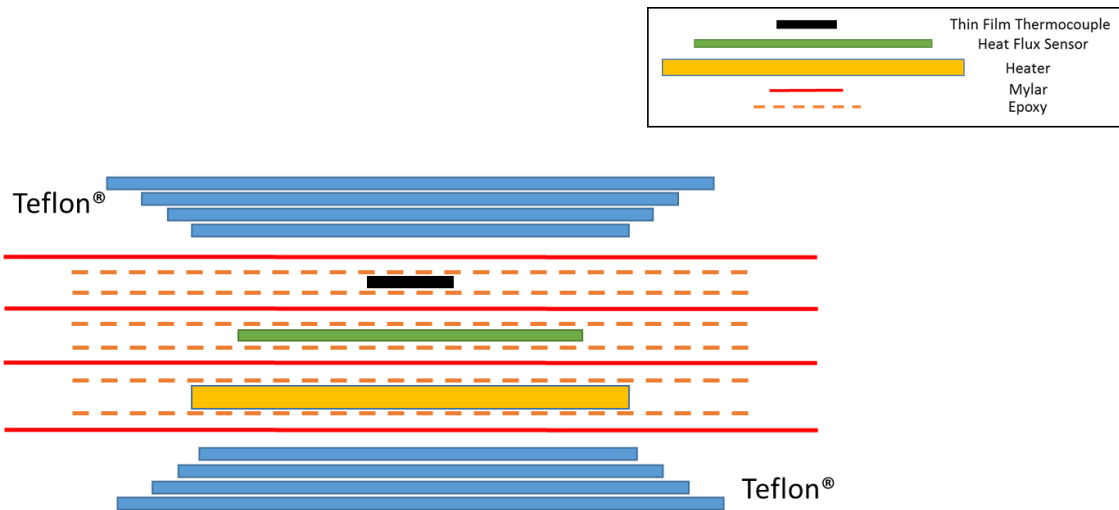


Figure 30. CHFT+ sensor layer assembly schematic

PHASE 1: Clean the Heat Press foundation and top surface

PHASE 2: Clean the heat flux sensor, thin film thermocouple, and resistive heater

PHASE 3: Assemble CHFT+ Sensor

- 1) Place the 4 bottom pieces of Teflon® on the bottom face of the hot press, followed by a sheet of Mylar. Press the Mylar, eliminating as many air bubbles as possible.

- 2) Using the epoxy brush, dab the epoxy onto the Mylar. Make sure you dab the epoxy in the area that has Teflon® directly under it. Epoxy use should be medium. Not too much and not too little.

- 3) Place the heater on the epoxy dabbed Mylar. MAKE SURE heater side without wire leads is upward. If desired, you may lightly dab the wired side with epoxy before placing it on the Mylar.

- 4) After placing heater, apply epoxy to the remaining heater surface. This is the surface without wire leads. Again, dabbing works best when applying the epoxy.

- 5) Place and press a sheet of Mylar on epoxy dabbed heater surface.

- 6) Repeat steps 2-5 for the heat flux sensor. AGAIN MAKE SURE heat flux sensor face with wire leads is the bottom surface. When placing heat flux sensor, make sure that it is placed exactly in the center of the heater. Meaning, the heat flux sensor should be aligned and centered on the heater surface. When sensor is placed on the epoxy surface, you can move it around slightly in order to determine ideal configuration.

- 7) Using the epoxy brush, dab a small amount of epoxy onto the Mylar. Make sure you dab the glue in the area that is above the center of the heat flux sensor.

- 8) Place the thermocouple above the desired area and determine its centrality with regard to the heat flux sensor. When aligned, slowly lower and press into Mylar.
- 9) Dab epoxy on top of thermocouple.
- 10) Place last Mylar sheet.
- 11) Apply Kapton[®] tape to all edges of exposed Mylar.
- 12) Place remaining pieces of Teflon[®] smallest first on top of one another.
- 13) Clamp press shut.
- 14) Open Press and remove top Teflon pieces.
- 15) Insure assembly is still aligned. If not, realign and re-do steps 12-14.
- 16) If aligned, replace Teflon pieces as done in step 12.
- 17) Clamp hot press shut.
- 18) Plug hot press into power outlet.
- 19) Set temperature to 160 C and turn off after 3 hours.
- 20) Let press cool down, in closed configuration, for 12 hours.
- 21) Slowly un-clamp and open press. You may feel some resistance.
- 22) Remove top Teflon[®] pieces.
- 23) Remove Kapton[®] tape and separate assembly from hot press.
- 24) Trim excess Mylar.
- 25) Test heat flux sensor, thermocouple and heater functionality.